PHOSPHATIDYLCHOLINE BIOSYNTHESIS IS INVOLVED IN AUTOPHAGY REGULATION IN RAS-TRANSFORMED INTESTINAL EPITHELIAL CELLS

by

Abdulmottaleb Zetrini

Submitted in partial fulfilment of the requirements
for the degree of Master of Science

at

Dalhousie University
Halifax, Nova Scotia
December 2016

DEDICATION PAGE

This work is dedicated to my family for their support and encouragement.

TABLE OF CONTENTS

LIST OF FIGURES

ABSTRACT

Ras oncogene increased CTP-phosphocholine cytidyltransferase α (CCTα) expression and phosphatidylcholine (PC) biosynthesis that were required for cell proliferation and survival. Ras-transformed intestinal epithelial cells (IEC-ras) have increased autophagy, which could be related to increased PC because phagophore membrane synthesis and PC synthesis take place at the endoplasmic reticulum (ER). Thus, we examined whether CCTα and PC synthesis are required for autophagy. RNAi silencing of CCTα in IEC-ras caused increased expression of p62 and LC3-II, indicative of impairment of autophagy. Decreased PC biosynthesis by choline depletion of IEC-ras also caused accumulation of p62/SQSTM1 and LC3-II, and inhibited cell growth. Choline depletion of non-malignant IEC cells had no effect on these parameters. Chloroquine did not alter p62/SQSTM1 or LC3-II in IEC-ras cultured in the absence of choline, indicating that autophagy is blocked before autophagosome-lysosome fusion. Autophagy was restored in choline-depleted IEC-ras34 by addition of lysophosphatidylcholine, which can be converted to PC. These data show that inhibition of PC synthesis is required to sustain autophagy and proliferation of IEC-ras.

LIST OF ABBREVIATIONS USED

AD	Alzheimer disease
Alfy	Autophagy-linked FYVE protein
Ambra-1	Autophagy/ Beclin 1 Regulator 1
Apaf-1	Apoptotic protease activating factor-1
Bcl-X_L	B-cell lymphoma-extra large
Bif-1	N-BAR-containing protein
Bip	Binding immunoglobulin protein
BNIP3	Bcl-2 adenovirus E1aa nineteen kDa interacting protein 3
BSA	Bovine serum albumin
CaMKKβ	Calcium-activated calmodulin-dependent kinase β
CEPT	Choline/ethanolamine phosphotransferase
CCT	CTP:phosphocholine cytidyltransferase
CDP	Cytidine diphosphate
CHO	Chinese hamster ovary
CHT	High affinity choline transporters
CF-DMEM	Choline-free DMEM
CK	Choline kinase
CL	Cardiolipin
CTL	Choline transporter-like proteins
CMA	Chaperone-mediated autophagy
CPT	Choline phosphotransferase
CQ	Chloroquine
Cyt C	Cytochrome C
DAG	Diacylglycerol
DISC	Death-inducing signalling complex
DMEM	Dulbecco's modified Eagle's medium
DRAM	Damage Regulated Autophagy Modulator 1

ECM	Extracellular matrix
EIF-4F	Eukaryotic initiation factor4E
ER	Endoplasmic reticulum
ERAD	ER-associated degradation
F4E-BP1	Factor 4E binding protein-1
FADD	Fas activating death domain
FBS	Fetal bovine serum
FIP200	Focal adhesion kinase family-interacting protein of 200 kD
FKBP12	FK506-binding protein of 12 kDa
GDP	Guanine diphosphate
GEFs	Guanine nucleotide exchange factors
GβL	G protein β-subunit-like protein
GTP	Guanine triphosphate
HIF-1	Hypoxia-inducible factor-1
IEC	Intestinal epithelial cells
IEC-ras	ras-transformed intestinal epithelial cells
Ire1	Inositol-requiring kinase 1
JNK	c-Jun N-terminal kinase
Keap1	Kelch-like ECH-associated protein 1
KIR	Keap1 interacting region
LAMP	Lysosomal membrane protein
LC3	Microtubule-associated protein
LD	Lipid droplet
LPCAT1	Lysophosphatidylcholine acyltransferase
lyso-PC	Lysophophatidylcholine
MAM	Mitochondria-associated membranes
MEM	α-minimal essential medium
MAPK	Mitogen-activated protein kinase
MTMR	Myotubularin
MTOC	Microtubule organising center

mTOR	Mammalian target of rapamycin
NAF-1	Nutrient deprivation autophagy factor-1
NFE2L2	Nuclear factor (erythroid-derived 2)-like 2
NLS	Nuclear localization sequence
OCT	Organic cation transporters
p62/SQSTM1	Sequestosome-1
PA	Phosphatidic acid
PAGE	Polyacrylamide gel electrophoresis
PARP1	Poly[ADP-ribose] polymerase 1
PAS	Phagophore assembly site
PB1	Bemp1 domain
PC	Phosphatidylcholine
PD	Parkinson disease
PDK1	phosphoinositide-dependent kinase 1
PE	Phosphatidylethanolamine
PEMT	Phosphatidylethanolamine methyltransferase
PI	Phosphatidylinositol
PI3K	Phosphoinositide 3-kinases
PIP3	Phosphatidylinositol-3,4,5-triphosphate
PKC	Protein kinase C
PLD1	Phospholipase D
PRAS40	Proline-rich Akt substrate of 40 kDa
PS	Phosphatidylserine
RAS	Rat sarcoma protein
Rheb	Ras homologue enriched in brain
ROS	Reactive oxygen species
SAM	S-adenosylmethionine
SDS	Sodium dodecyl sulphate
shRNA	Short hairpin RNA
SIN1	SAPK- interacting protein

S6K1	Ribosomal protein S6 kinase-1
SREBP	Sterol regulatory element-binding protein
TECRPR1	Tectonin domain-containing protein 1
TG	Triglyceride
TSC	Tuberous sclerosis
TRAF6	Tumor necrosis factor associated receptor -6
UBA	Ubiquitin association domain
ULK	Unc-51 like kinases
UPR	Unfolded protein response
UVRAG	UV Radiation Resistance Associated
VLDL	Very low-density lipoprotein
Vps34	Vacuolar protein sorting 34
VSVG	Vesicular stomatitis virus glycoprotein
WIPI	WD repeat domain phosphoinositide-interacting
ZZ	Zinc finger domain

ACKNOWLEDGEMENTS

This work could not have been accomplished without many people. I would like to thank my supervisory committee members Dr. Catherine Too and Dr. Barbara Karten for their suggestions and valuable comments towards my project. I would like to acknowledge all the members of the Atlantic Research Centre. Special thanks to the Ridgway lab members past and present, as well as Byong Hoon. Particular mention goes to Kexin Zhao for his recommendations throughout my work, and Rob Douglas for his patience and consistent maintaining of cell cultures.

I would like to acknowledge the Ministry of Higher Education in Libya for sponsoring me in my master's program. This work was funded by The Canadian Institutes For Health Research (CIHR).

Finally, I would like to thank my supervisor Dr. Neale Ridgway for giving me a chance to join his lab and pushing me to do my best, which helped me to develop my knowledge regarding scientific research. I appreciate all the patience and criticisms over the last two years.

CHAPTER 1 INTRODUCTION

1.1 The role of phospholipids and phosphatidylcholine in cellular function

Cell membranes composed of proteins, phospholipids, glycolipids, cholesterol and sphingolipids separate intracellular compartments (i.e. organelles) and act as a barrier to the external environment. In eukaryotes, phosphatidylcholine (PC), phosphatidylserine (PS), phosphatidylethanolamine (PE), phosphatidylinositol (PI) and cardiolipin (CL) are the main phospholipid components of cell membranes (1). In addition to a structural role in membranes, phospholipids are involved in many other functions. For example, PS, which comprises 5% of membrane phospholipids, is required for apoptosis (2). In non-apoptotic cells, flippases catalyzes the transport of PS from the outer to the inner leaflet of the plasma membrane. During apoptosis, flippases are inactivated and PS is exported to the extracellular surface of the plasma membrane where it acts as a recognition signal for phagocytosis (3). PI, which makes up 5-15% of total membrane mass, is phosphorylated at three sites in the inositol headgroup, forming seven different phosphorylated PIs, with specific signaling functions (4). PE, which is the second most abundant phospholipid in cell membranes (25%), has a conical shape because of the small head group and induces negative curvature in membranes (5). CL, which is almost exclusively in the inner mitochondrial membrane, is also involved in apoptosis regulation (6). CL associates with cytochrome c (cyt c) and electron transport complexes III to IV to facilitate oxidative phosphorylation. When apoptosis is induced, CL is oxidized by the CL-specific peroxidase activity of CL-bound cyt c, resulting in secretion of cyt c from the

mitochondria, formation of the apoptosome, and activation of the caspase proteolytic cascade (6).

The most abundant phospholipid in mammalian membranes and secreted complexes (i.e. lipoproteins) is PC. In eukaryotes, PC comprises 40-60% of membrane lipids. Moreover, PC is also secreted in complex with other lipids and proteins in the form of lipoproteins, lung surfactant and bile (8). PC is composed of a phosphocholine head group at the *sn-3* position of glycerol and two long-chain fatty acyl groups esterified at the *sn-1* and *sn-2* positions (8) and is a precursor for signalling molecules produced by different phospholipases (8). For example, phospholipase A2 hydrolyzes the sn-2 fatty acid to release arachidonic acid, which is used for the synthesis of leukotrienes and prostaglandins, which are inflammatory lipid mediators (9). Phospholipase C cleaves the phosphocholine headgroup from PC to form diacylglycerol (DAG), an activator of protein kinase C (PKC) (10). Hydrolysis of PC by phospholipase D (PLD) yields phosphatidic acid (PA), which is a vital cellular lipid that acts as a precursor for all acylglycerol lipids (11).

During the late G2/M phase of cell division, PC synthesis is increased to double membrane mass that is necessary for cell division (7). The subject of my graduate research was to investigate how the high rate of PC synthesis in cancer cells promotes proliferation and evasion of apoptosis. Autophagy is a pro-survival pathway for cancer cell that is dependent on lipid signalling and membrane expansion (discussed later in more detail). Thus, I investigated whether activity of the rate-limiting enzyme in PC synthesis and choline availability promote cell survival through an autophagy-related mechanism.

1.2 Phosphatidylcholine synthesis and regulation

The main source of the quaternary amine choline is from dietary sources such as eggs, liver, wheat germ and milk, where choline is found in free form, in lipids or other water-soluble metabolites (i.e. glycerophosphocholine, phosphocholine, sphingomyelin) (14). Choline can also be synthesized *de novo* by the successive methylation of PE by phosphatidylethanolamine methyl transferase (PEMT). Choline is a precursor for acetylcholine, a neurotransmitter that is important in sleep, memory and learning (12). However, the majority of choline is incorporated into PC and sphingomyelin (13). The daily average intake of choline for males and females is 8.4 mg/kg and 6.7 mg/kg, respectively (15). One study suggested that pregnant women depend more on the *de novo* choline biosynthesis pathway by estrogen-dependent upregulation of PEMT (14).

1.2.1 PC synthesis by PE methylation

PE methyltransferase (PEMT) catalyzes the synthesis of PC through three successive methylations of the PE amino group to form the quaternary nitrogen (Figure 1.1) (16). PEMT uses S-adenosylmethionine (SAM) as a methyl group donor (16). PEMT activity is regulated by the availability of the substrates, SAM, PE, and the product S-adenosylhomocysteine. PEMT is expressed primarily in the liver, and generates 30% of hepatic PC, with the remainder 70% coming from the CDP-choline pathway (18). Differentiated adipocytes express significant amounts of PEMT that is required for lipid droplet biogenesis, but most other tissues express almost undetectable levels of enzyme activity or protein (19). In hepatocytes, two PEMT isoforms exist; PEMT1 is localized on

the endoplasmic reticulum (ER) (18), while PEMT2 is on mitochondria-associated membranes (MAM), a subdomain of the ER that forms tight contact sites with the mitochondria (20).

When fed a chow diet containing choline *PEMT* $^{-/-}$ mice were viable. However, *PEMT* $^{-/-}$ mice fed a choline-free diet died within 3 days due to steatosis and liver failure, a consequence of 50% reduction in hepatic PC levels (21). These results indicate that PEMT is the sole source of choline in animals when a dietary choline is restricted, allowing the animals to survive in the absence of dietary choline.

PEMT $^{-/-}$ mouse hepatocytes secreted decreased very low-density lipoproteins (VLDL) compared to the wild type mice (22). Surprisingly, impairment of *de novo* PC and choline biosynthesis in PEMT $^{-/-}$ mice protected them from obesity and insulin resistance caused by a high-fat diet. Wild-type mice gained weight and experienced insulin resistance when they were fed a high fat diet, while *PEMT* $^{-/-}$ mice were totally protected from obesity and were insulin-sensitive when fed the same diet (23). Increasing the choline content of the diet reversed this protection.

1.2.2 CDP-choline pathway for PC synthesis

Eugene Kennedy identified the CDP-choline pathway for PC synthesis in 1956 (6). Unlike PEMT, the CDP-choline pathway is found in all eukaryotic cells including hepatocytes. The PC made by the CDP-choline pathway is enriched in medium chain saturated fatty acids, while the PEMT pathway makes PC rich in long-chain polyunsaturated fatty acids (24).

1.2.3 Enzymatic steps in the CDP-choline pathway.

Choline is a positively charged quaternary amine that is membrane impermeable. Uptake of choline into cells is mediated by transporters located in the plasma membrane (Figure 1. 1). Three different types of choline transporters have been identified: high affinity sodium-dependent choline transporters (CHT1), intermediate-affinity sodium independent choline transporter like proteins (CTLs) and low affinity organic cation transporters (OCTs). CHT1 is expressed in the central nervous system and is involved in choline uptake for acetylcholine biosynthesis (25). CTLs are the main transporters that mediate choline uptake for PC biosynthesis and are encoded by five genes (CTL1-5). CTL1 appears to be the major choline transporter in this group for phospholipid biosynthesis.

OCTs are sodium-independent, low affinity organic cation transporters that are found in most cells and are comprised of five members: OCT1, OCT2, OCT3, OCTN1 and OCTN2 (26). OCT1 is expressed mainly in the liver, whereas OCT2 is found in the kidney and some parts of the brain. OCT3 is expressed in multiple organs in the body such as intestine, hearth, brain and abundantly in placenta (26). Each group of choline transporters exhibits different sensitivity to the choline transport inhibitor hemicholinium-3. While CHT1 and CTL1 are sensitive and partially sensitive to hemicholinium-3, respectively, the OCTs are insensitive (27).

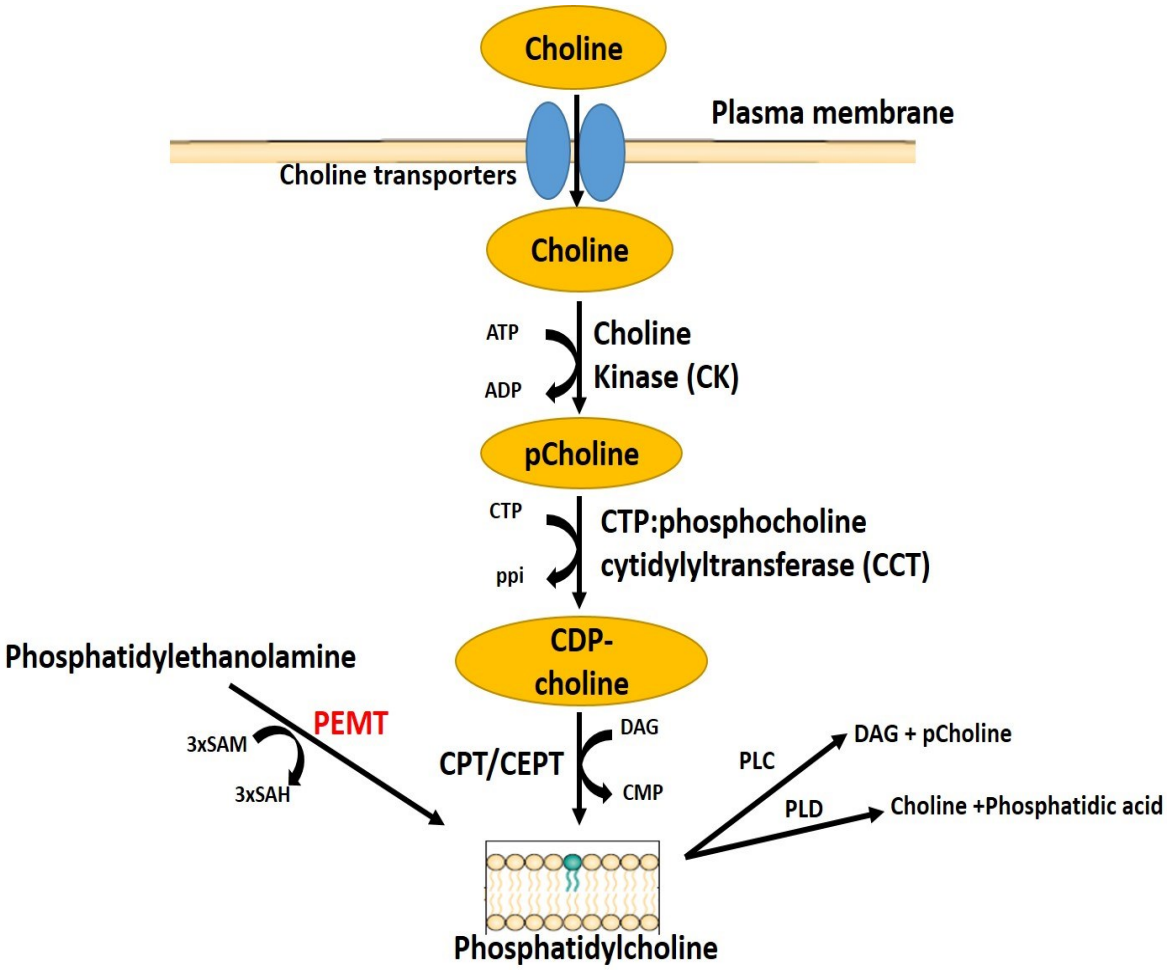

Figure 1.1: Phosphatidylcholine biosynthesis by the PEMT and the CDP-choline pathways. This scheme shows the metabolic intermediates and the product of the PEMT and the CDP-choline pathways and the enzymes involved.

Choline kinases are cytosolic enzymes that catalyze the ATP dependent phosphorylation of choline to phosphocholine (**Fig. 1. 1**). Three choline kinases isoforms (CKα1, CKα2 and CKβ) are expressed in mammalian cells and are encoded by the *Chkα* and *Chkβ* genes (28). Choline kinase isoforms are active homodimers or heterodimers. CKα plays a crucial role in early development since mice lacking CKα die at an early stage of embryogenesis (29). Ras-oncogene up-regulates CKα expression in mouse fibroblast and enhances the production of phosphocholine, which promotes cancer growth (30) and resistance to 5-fluorouracil (31). Therefore, targeting CKα might be a tool to control cancer growth and invasiveness. CKβ seems to be non-essential and have overlapping function with CKα since knockout mice survive to maturity (32). However, CKβ is highly expressed in hind-limb muscle, and $CK\beta^{-/-}$ mice develop muscular dystrophy (32). The precise role of CKβ in muscle function is unknown.

CTP:phosphocholine cytidylyltransferase (CCT) catalyzes the rate-limiting conversion of phosphocholine and CTP to CDP-choline and pyrophosphate (Figure 1. 1). The *Pcyt1a* and *Pcyt1b* genes encode CCTα and CCTβ isoforms, respectively (33). CCTα consists of four domains; a nuclear localization sequence (NLS), an α-helical membrane binding domain, a catalytic domain and a phosphorylation domain (34). CCTβ isoforms (CCTβ1, CCTβ2 and CCTβ3) do not contain a NLS, and CCTβ1 does not have the phosphorylation domain (33). CCTβ3 is similar to CCTβ2 but does not contain the amino terminal 28 amino acids, CCTβ isoforms are found in the cytoplasm and ER, and expressed at lower levels compared with CCTα (33, 35).

CCTβ is highly expressed in brain and gonadal tissues. CCTβ2 $^{-/-}$ mice have defects in gonadal development and fertility but no overt neurological symptoms (36).

Induction of differentiation in rat adrenal medulla PC12 cells and Neuro2a by nerve growth factor and retinoic acid, respectively, increased the activity and expression of CCTβ2, but not CCTα, suggesting that CCTβ2 is involved in increased PC production during differentiation for neurite growth. Also, reduction of CCTβ expression caused decreased growth and proliferation of PC12 cells (36).

CCTα is expressed in all mammalians tissues, especially liver and lung (27). In lung, increased CCTα and PC are required for secretion of lung surfactant, which is composed of 80% PC. Surfactant is secreted by lung epithelial cells and is composed of phospholipid and surfactant proteins, important for respiration (37). Knockout of CCTα decreases the number of microvilli and secretory bodies that make surfactant (38).

CCTα was up-regulated 5-10 fold in ras-transformed intestinal epithelial cells and its silencing decreased proliferation of these cells, and induced anoikis after detachment from the ECM (39). Another study found that inhibition of CCT leads to inhibition of PC biosynthesis and induction of apoptosis (40). However, the mechanism of induction of anoikis (in detached cells) and apoptosis (in attached cells) is not known.

CCTα is localized to the nucleus by a stretch of 5 basics residues in the N-terminus that when introduced into β-galactosidase also promotes its import into the nucleus (41). CCTα is localized to the nucleus in most cells, and transported out of the nucleus when cells are treated with lipid activators such as oleate (42). However, in cells that require high amounts of PC such as differentiating B-cells, CCTα is predominantly localized in the cytoplasm to activate the synthesis of PC (42). Expression of CCTα lacking an NLS in CCTα-deficient Chinese Hamster Ovary (CHO MT58) cells restored

the synthesis of PC, the growth and survival of these cells (41), indicating that NLS is not required for activity of CCTα.

The NLS of CCTα contains a site for caspase 3 cleavage at the $TEED_{20}$ motif, which is C-terminal to the NLS (43). Induction of apoptosis by farnesol in CHO cells causes the translocation of CCTα to nuclear envelope and cytoplasm, and caspase cleavage of the CCTα NLS. CCTα with the TEED cleavage site mutated still exported from the nucleus after farnesol treatment, implying that removal of NLS is not required for nuclear export but could be required for reimport, effectively trapping CCTα in the cytoplasm (43).

The catalytic domain (amino acid 73-236) is highly conserved in mammalian CCTα and CCTβ (44). CCTα is a homodimer and the site of dimerization is at amino acids 139-145 in the catalytic domain (45). There are a number of key motifs that are essential for catalysis and substrate binding. A R196K mutation in the RTEGISTS motif (amino acids 196-203) results in reduction of CTP binding by 23-fold and V_{max} by 3-fold (46), indicating a role in substrate binding and catalysis. HXGH (amino acids 89-91) is the catalytic motif in CCTα (47). The two histidine residues are needed for transition state stabilization, and mutation of either histidine reduces CCTα V_{max} activity (46). However, the substrate K_m did not change in these histidine mutants, suggesting that HXGH motif is not involved in substrate binding.

CCTα is found as an inactive soluble form and an active membrane-bound form. Interaction with membranes is controlled by Domain M (amino acids 236-300), a segment that regulates activation of catalysis by membrane interaction (48, 49). Domain M inhibits catalysis in soluble inactive CCTα, but after binding to membranes, the

inhibitory effect is relieved (50). When domain M binds to membranes, it causes a conformational change that results in an 80-fold increase in catalytic activity of CCTα (46). Deletion of domain M from CCTα resulted in no lipid activation, reducing the activity by 90%, and decreasing the fraction of membrane-bound enzyme.

The C-terminal phosphorylation domain (amino acids 315-367) contains 16 serine phosphorylation sites in human CCTα (51). Mutation of the 16-serine residues to alanine increased CCTα membrane binding and PC synthesis by 10- and 2-fold, respectively. CCTα is dephosphorylated during late G1 phase and is activated, but during G0 and M phases CCTα is phosphorylated and less active. This means that increased catalytic activity is correlated with decreased phosphorylation (52). In addition, deletion of the phosphorylation domain increases catalytic activity of CCTα and it becomes insensitive to lipid activators (53). The relationship between phosphorylation status and CCTα stimulation indicates that phosphorylation reduces the affinity of CCTα for membranes.

The last step in CDP-choline pathway is catalyzed by CDP-choline: diacylglycerol cholinephosphotransferase (CPT). CPT transfers the phosphocholine moiety from CDP-choline to diacyglycerol to produce phosphatidylcholine. CPT is mainly localized in the Golgi apparatus (54), and its mRNA is highly expressed in the small intestine and testis (55). The activity of CPT is controlled by the availability of the substrates, and increasing the expression of CPT does not change the rate of PC synthesis. Choline/ethanolamine phosphotransferase (CEPT), which is found on the ER (54), is also involved in CDP-choline pathway. Unlike CPT, CEPT uses both CDP-ethanolamine and CDP-choline to make PE and PC, respectively. CEPT mRNA is abundantly present in spleen, intestine, heart and colon (55). Under normal conditions,

neither CEPT nor CPT activity is rate-limiting, but they can become rate-limiting when DAG is restricted (56).

Studies have investigated the importance of PC made by the PEMT versus CDP-choline pathways. CHO MT58 cells express a temperature-sensitive CCTα allele that causes blockage of the CDP-choline pathway at 40°C and cell death. These cells can be rescued by expression of PEMT. However, MT58 cells cultured in fatty acid-deficient medium at 40°C were not rescued by PEMT expression (57). These data suggest that the PEMT pathway cannot substitute for the CDP-choline pathway in MT58 cells under specific conditions of fatty acid limitation that restricts the synthesis of sufficient PE substrate. However, in liver-specific CCTα knockout mice, the PEMT pathway is able to supply sufficient PC for liver (57). These studies suggest that the CDP-choline pathway is a vital pathway for PC synthesis in most tissues while the PEMT pathway plays a significant role only in the liver.

1.3 Oncogenic regulation of phosphatidylcholine biosynthesis

1.3.1 Ras signaling

Ras (rat sarcoma protein) is a signal transducing small GTPase that control cell proliferation and differentiation. The GTPase family consists of about 170 members and there are 3 ras-related members (H-ras, K-ras and N-ras). Ras can be in an inactive GDP-bound state, or an active GTP-bound state. The GDP/GTP ratio is regulated by GTPase-activating proteins (GAPs) and guanine nucleotide exchange factors (GEFs) (58). Ras is a downstream effector for many tyrosine kinase receptors such as EGF, insulin, and

platelet-derived growth factor. Stimulation of these receptors activates the conversion of GDP to the active form GTP, thus promoting cell growth and proliferation.

Enzymes of the CDP-choline pathway are affected by the ras oncogene. For instance, CK expression and phosphocholine are increased in H-ras-transformed NIH3T3 fibroblasts (59). A study found that ras signalling can lead to suppression of CCT activity by c-Jun N-terminal kinase (JNK). JNK is highly expressed in murine lung, and causes phosphorylation of CCTα, subsequently reducing CCTα activity by 40% and PC synthesis by 30% (60). On the other hand, oncogenic H-ras increases transcription of CCTα via the stimulation of the MAPK pathway and a transcription factor SP3 (61). MAPK modulates the expression of sterol regulatory element binding-proteins (SREBPs), which then activate membrane translocation of CCTα and increase enzyme activity through enhanced production of fatty acids (61). It seems that one mechanism for ras oncogene pathogenicity is through increasing the synthesis of PC, which may be essential for cancer cells to make membranes and proliferate.

1.3.2 The PI3K-AKT pathway and regulation of CDP-choline pathway

Phosphoinositide 3-kinases (PI3K) are a large family of lipid enzymes that phosphorylate the 3-hydroxyl group of PI at the cytosolic surface of the plasma membrane. In mammalian cells, class I, class II, and class III PI-3Ks have been identified. Class I is divided into class IA and class IB, and are implicated in cancer (62). In mammals, three class II members have been identified: the ubiquitously expressed PI3K-C2 α and PI3KC2-β, and the liver-specific PI3K-C2γ, all play a role in regulating vesicular trafficking (63). Class III includes only vacuolar protein sorting 34 (Vps34),

which is involved in autophagy initiation. The PI3K-AKT pathway is commonly activated in human cancers and mutation in PI3K components and/or tumor suppressor genes such as *PTEN* promote growth and survival of cancer cells (64). Suppression of the PI3K-AKT pathway results in blockage of choline uptake, subsequently preventing the conversion of choline into phosphocholine in lung-adenocarcinoma cell lines (65). In addition, knockdown of CKα using siRNA can inhibit cell proliferation by decreasing the activity of PI3K-AKT signalling (66). This provides good evidence that PI3K-AKT pathway is involved in up-regulation of CDP-choline pathway to enhance tumour growth. It seems that targeting PC biosynthetic enzymes affects cancer cells growth and survival.

1.4 PC synthesis and apoptosis

1.4.1 Programmed cell death: apoptosis

Apoptosis (programmed cell death) is important for immune system function, embryonic development, and regulation of normal cell proliferation (67). Dysregulation of apoptosis causes impaired organ formation, autoimmune diseases, neurodegenerative disease and cancer (67). Apoptosis is triggered by the initiator and effector caspases, which are present in inactive procaspase form. When initiator caspases such as caspase 2, 8, 9 and 10 are activated by a pro-death signal, such as Fas activating death domain (FADD) and apoptotic protease activating factor-1 (Apaf-1), initiator caspases bind to and proteolyze effector caspases, leading to their activation and breakdown of the cellular components (68).

Apoptosis can occur via the intrinsic and extrinsic pathways. The intrinsic pathway is triggered by internal stimuli such as environmental stress and DNA damage that lead to cyt *c* release from mitochondria (4). Cyt *c* recruits Apaf-1 to form an apoptosome, which activates caspase 9, and subsequently activation of effector caspases, for example caspase 3 (69). The extrinsic pathway is mediated by ligands such as Fas-L that activate death receptors to recruit FADD, followed by procaspase 8 and formation of the death-inducing signalling complex (DISC). This results in activation of caspase 8 and eventual activation of effector caspases (70).

The requirement of cancer cells for PC indicates that PC biosynthesis may be a target of apoptosis. Disruption of PC synthesis in PC12 cells (cell lines derived from a pheochromocytoma of the rat adrenal medulla) through choline deprivation, and inhibition of CKα in HeLa cells by RNAi resulted in decreased PC synthesis and apoptosis (71). Furthermore, inhibition of CPT in human lung adenocarcinoma can induce apoptosis (72). Similarly, disruption of PC synthesis by thermo-denaturation of CCTα in CHO-MT58 cells leads to reduction in PC synthesis, induction of apoptosis, and growth arrest in G1 phase (73). These results indicate that disruption of PC biosynthesis causes apoptosis, and that cancer cells that are apoptosis resistant could drive PC synthesis to make membranes for cell cycle progression and proliferation.

1.4.2 Detachment-dependant apoptosis: anoikis

Detachment of epithelial cells from the extra-cellular matrix (ECM) causes cell death by a mechanism called anoikis (74). Detachment of epithelial cells from ECM leads to dysregulation of integrins, transmembrane adhesion receptors on epithelial cells (75).

This causes alteration in the activity of kinases such as Raf and p38 MAPK, and changes the activity of downstream effectors implicated in anoikis such as Bax and B-cell lymphoma/ leukemia-2 (Bcl-2) (76-78). In normal cells, loss of integrin function after detachment induced anoikis via upregulating Fas ligand by a p38 MAPK-dependent mechanism (76).

H-ras oncogene was found to inhibit anoikis through multiple pathways, for example downregulation of pro-apoptotic proteins Bim, and upregulation of anti-apoptotic proteins, such as B-cell lymphoma-extra-large (Bcl-X_L) (79, 80). In addition, H-ras promotes proliferation by downregulating beclin-1, subsequently blocking autophagy (81).

The CDP-choline pathway is linked to anoikis resistance in H-ras-transformed intestinal epithelial cells (IEC-ras) (82). In adherent IEC-ras, the expression and activity of CCTα, and PC hydrolysis were increased compared to normal cells. In addition, upon detachment, the IEC-ras-transformed cells resist anoikis, and CCTα phosphorylation and cytosolic enzyme activity were increased (82). Increased PC synthesis in detached IEC-ras was reduced after CCTα knockdown. This shows that increased PC synthesis in IEC-ras is involved in anoikis resistance after detachment from the ECM (82). *How increased PC synthesis contributes to anoikis resistance was a major focus of my thesis research.*

1.5 Autophagy and lipid metabolism

1.5.1 Types of autophagy

A major component of my research involved investigating the role of PC in autophagy, especially the proliferation of ras-transformed cells. Autophagy is a cellular catabolic process where components of the cytoplasm and organelles are encapsulated in double membrane autophagosomes and transported to lysosomes for degradation. Autophagy helps to maintain energy and nutrient homeostasis during cellular differentiation, tissue remodeling and cell death (83, 84). Multiple signals, such as lack of nutrients, hypoxia and unfolded protein response can induce autophagy. In mammalian cells, three forms of autophagy have been described: macroautophagy, microautophagy and chaperone-mediated autophagy (83, 84). In macroautophagy, which is the focus of my project, (referred to autophagy), autophagosomes engulf damaged organelles, long-lived proteins, and pathogens are transported to the lysosome. The autophagosome fuse with the lysosome to form autolysosome where autophagic cargo is degraded. The degraded products are recycled for use during starvation as substrates for new macromolecules (83).

Microautophagy, is a non-selective degradative process that is characterized by the engulfment of the cytosolic contents by a direct invagination of the lysosomal membranes into tubulovescular structures (83). Chaperone-mediated autophagy (CMA) is a selective lysosomal pathway that involves specific protein degradation. CMA degrades 30% of cytosolic proteins when cells are exposed to conditions of prolonged nutrients

starvation (83, 84). The microautophagy and CMA These will not be discussed in my thesis, and the focus is only on macroautophagy.

1.5.2 Induction of autophagy and phagophore formation

Autophagy involves specific steps of 1) induction and phagophore initiation, 2) phagophore expansion and elongation, 3) autophagosome formation, 4) autophagosome-lysosome fusion and 5) breakdown of the cargo (**Fig. 1. 2**). The source of membrane for forming an autophagosome is still controversial but could be derive *de novo* from the ER or the MAM. One study found that the rough ER surrounds the outer and inner surfaces of the pre-autophagosomal structure (85, 86). In addition, blocking autophagosome maturation through overexpression of Atg4B, which causes a defect in autophagosome formation, leads to accumulation of ER-associated autophagic structures (86, 87). This suggests that the ER is involved in autophagy regulation.

The first step in autophagy is the formation of the phagophore (also called the isolation membrane). In normal conditions, the basal level of autophagy is very low. When cells undergo stress, autophagy is induced to provide energy. In yeast, the serine/threonine protein kinase TOR (target of rapamycin) inhibits Atg1, another serine/threonine kinase, under conditions of nutrient availability (88). During starvation, TOR is inhibited, resulting in Atg1 activation, which forms a complex with Atg13 and Atg17. The Atg1-Atg13-Atg17 complex enhances the recruitment of several Atg proteins to the phagophore assembly site (PAS), and initiates the formation of autophagosomes (89). In mammalian cells, there are two homologs of Atg1, Unc-51 like kinases 1 and 2 (ULK1 and ULK2). After starvation, the focal adhesion kinase family-interacting protein

of 200 kDa (FIP200), a mammalian homolog of yeast Atg17, binds with Atg13 and ULKs, forming a complex localized on the phagophore. Mammalian Atg13 and FIP200 are phosphorylated by ULKs. The latter undergo autophosphorylation, causing autophagy induction (90). Atg101, which was identified as a component of the ULKs-Atg13-FIP200, is also required for autophagy through binding and stabilizing Atg13 (91). The formation of the autophagosome also requires a complex of vacuolar protein sorting 34 (Vps34), a myristoylated serine/threonine kinase (p150), mAtg14 and beclin1 (92, 93). Vps34 activity is increased by its interaction with Beclin1 (94). Multiple proteins interact with beclin1, and disruption of this interaction impairs autophagosome formation. Autophagy/ Beclin 1 Regulator 1 (Ambra-1), UV Radiation Resistance Associated (UVRAG) and N-BAR-containing protein (bif-1) bind to beclin1 to induce autophagy, while the interaction of the Bcl-2 or bcl-x_L, antiapoptotic proteins, with beclin1 inhibits autophagy (95). Recently, a new component of the PI3K complex has been identified; nutrient deprivation autophagy factor-1 (NAF-1) (96). NAF-1 binds with Bcl-2 and enhances the interaction of beclin1 with Bcl-2, whereas NAF-1 silencing diminishes Bcl-2-beclin1 interaction and induces autophagy (96). Under starvation condition, JNK1 is activated and leads to Bcl-2-beclin1 dissociation, hence inducing autophagy (97).

1.5.3 Phagophore elongation and autophagosome maturation

Two ubiquitin-like reactions, Atg12-Atg5-Atg16 and Atg8/LC3-PE, take place during the expansion of the autophagosomal membtane (98). Atg12 is stimulated by the E1-activating enzyme (Atg7), transferred to the E2 activating enzyme (Atg10), bonds covalently to an internal lysine residue of Atg5 through its carboxyl-terminal glycine (99). The Atg12-Atg5 complex interacts with Atg16 via the coiled–coil domain of Atg16

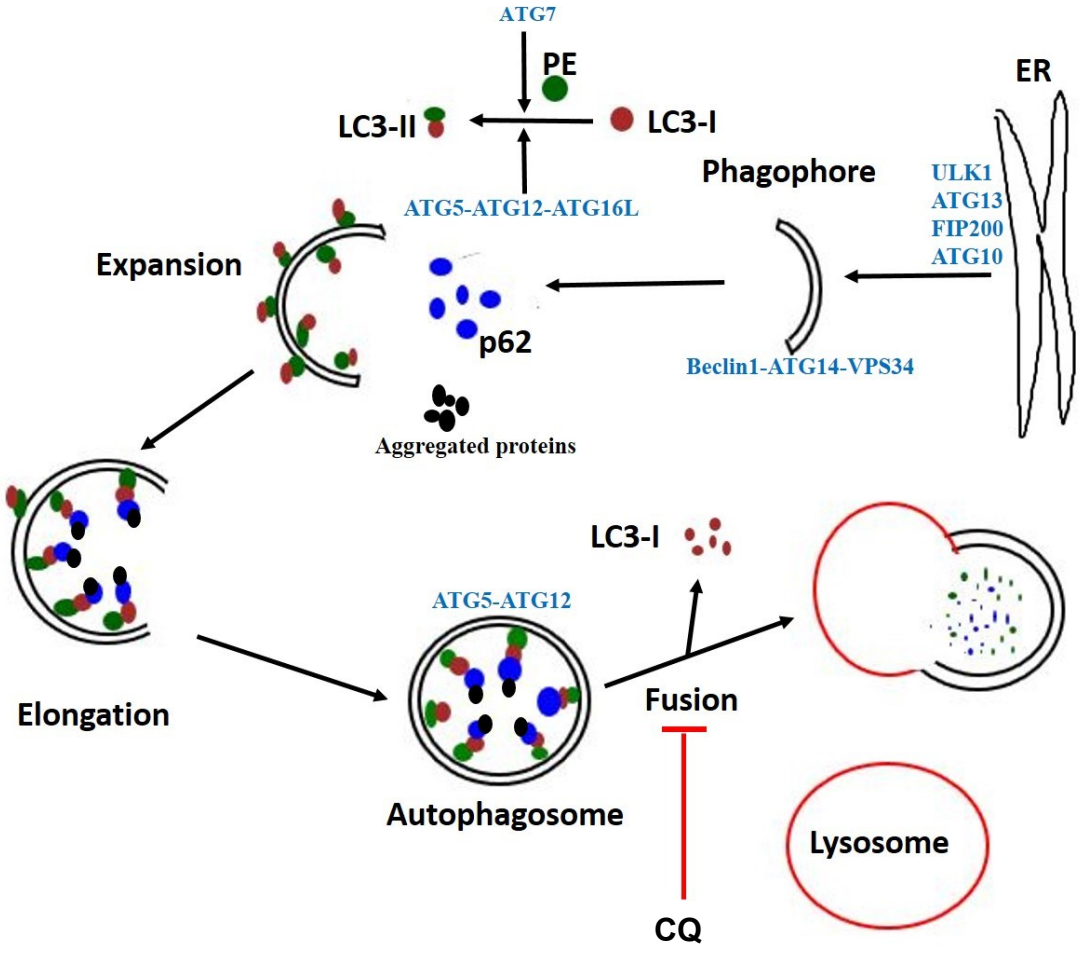

Figure 1-2: Steps of the autophagy process. Autophagy is initiated with the formation of an isolation membrane (phagophore), which is mediated by the ULK complex (ULK1, ATG13, FIP200 and ATG101). Phagophore nucleation requires the beclin1-ATG14-VPS34 complex. During phagophore elongation, ATG7 aids in LC3-I lipidation with PE to form LC3-II complex. ATG5-ATG12-ATG16L complex is required for phagophore elongation. p62 binds with LC3-II and other aggregated proteins and allows packaging in the autophagosome. Finally, the autophagosome fuses with the lysosome for degradation of the autophagosomal contents. p62 is degraded and LC3-II is delipidated to LC3-I. Chloroquine (CQ) blocks fusion of the autophagosome with the lysosome.

and forms the Atg12-Atg5-ATg16 tetramer complex (100).Once the autophagosome is completed, Atg16 leaves the complex and the Atg12-Atg5 conjugate attaches to the surface of the autophagosome, which is commonly used as a marker for autophagy. Interestingly, Atg16 is implicated in Crohn's disease, inflammatory bowel disease in human. Atg16-deficient macrophage had high amounts of inflammatory cytokines (101). In addition, Atg16 regulates Paneth cells, a special type of epithelial cells that secret antimicrobial peptides and other proteins important for the intestinal environment (102). These findings are similar to Crohn's patients with mutation in Atg16

The second ubiquitin-like reaction involves the microtubule-associated protein light chain3 (LC3), which is encoded by the mammalian homolog of Atg8 (98). Atg4 cleaves LC3 at the carboxyl terminal, forming the cytosolic isoform LC3-I (103). LC3-I is activated by Atg7, transferred by Atg3 and conjugated to PE through an amide bond to form LC3-II (104). Unlike Atg12-Atg5-Atg16 complex, the LC3-PE complex remains on the surface of the completed autophagosome until the lysosomes fuse, after which the PE is removed from LC3-II by Atg4 and recycled (105). It has been established that the two ubiquitin-like complexes interact with each other. The Atg-12-Atg5-Atg16 complex enhances the lipidation of LC3-I by transferring LC3-I to the site of lipidation for conjugation with PE. The association of LC3-II with either the inner or outer surfaces of autophagosome makes it a widely used marker for autophagy.

p62/SQSTM1 (p62/SQSTM1), is a multifunctional protein that consists of six domains: the N-terminal phox and Bemp1 domain (PB1), tumor necrosis factor associated receptor-6 (TRAF6) binding domain (TB), LC3 interacting region (LIR), the ubiquitin association domain (UBA), zinc finger domain (ZZ) and Kelch-like ECH-

associated protein 1 (Keap1) through a Keap1 interacting region (KIR) (106). The PB1 (amino acids 20-102) allows p62/SQSTM1 to oligomerize, which is necessary for degrading autophagy substrates (107). The TB domain (amino acids 225-251) helps p62/SQSTM1 to bind with TRAF6 for NFKB signaling (108). The ZZ domain (amino acids 122-167) is found in the nucleus where it is implicated in regulation of transcription through binding to nuclear transcription factors (109). LIR domain (amino acids 321-342) is essential for binding of p62/SQSTM1 with LC3 and cargo degradation during autophagy (110). The UBA (amino acids 389-434) mediates p62/SQSTM1 binding to ubiquitin-tagged proteins and damaged organelles (111).

p62/SQSTM1 is implicated in signal transduction, aging, neurodegenerative diseases, oxidative stress response and in degradation of protein aggregates and organelles through autophagy (112). In addition, p62/SQSTM1 is mutated in human Pagets disease of bone, a chronic disease characterized by increased bone turnover (113). Similarly, knockout of p62/SQSTM1in mice caused an impairment of osteoclastogenesis (114).

Accumulation of protein aggregates is the main feature of neurodegenerative diseases such as Alzheimer (AD), Parkinson (PD) and Huntington (115). p62/SQSTM1 is found in all protein aggregates causing these diseases, suggesting a role in their formation or clearance (116). Inactivation of p62/SQSTM1 resulted in AD-like phenotype in a mouse model (117). In addition, the expression of p62/SQSTM1 is reduced in the brain of AD patients (118). In PD, impaired mitochondrial functions and oxidative stress are the main characteristics of the disease (115). p62/SQSTM1 has been found to protect the brain by enhancing the activity of the transcription factor Nuclear factor (erythroid-

derived 2)-like 2 (NFE2L2) and degrading damaged mitochondrial and aggregated proteins (119). Deletion of p61/SQSTM1 is correlated with reduction of NFE2L2 activity in neurons, increased oxidative stress (118). Altogether, p62/SQSTM1 has a protective role in neurodegenerative diseases.

In autophagy, p62/SQSTM1 is one of the autophagy receptors that promotes degradation of cargos by three different mechanisms; 1) p62/SQSTM1 recruits ATG proteins to early sites of autophagosome formation via PB1 domain (107), 2) p62/SQSTM1 associates with ubiquitinated proteins, forming ubiquitinated cargos through the UBA domain and directs them to lysosome for degradation (120), 3) p62/SQSTM1 binds with LC3-II via LIR for delivery to autophagosomes (121). Therefore, p62/SQSTM1and LC3-II are commonly used as a marker of autophagy. Suppression of autophagy causes an increase in p62/SQSTM1 level, while decreased p62/SQSTM1 levels are associated with autophagy activation (122).

1.5.4 Autolysososme formation and contents degradation

After the formation of the autophagosome, it transports bidirectionally to the microtubule organising center (MTOC), where lysosomes are concentrated (123). Dynein motor proteins mediate this movement towards the MTOC, since inactivating mutations in dynein suppressed clearance of autophagosomal contents (124). The fusion of the autophagosome with the lysosome requires proteins such as ESCRT, SNAREs, Rab7 and the lysosomal membrane protein (LAMP-2) (125). In addition, UVRAG, a beclin1 interacting protein, interacts with the Vps34 protein and activates Rab7, resulting in autolysosome formation (126). Autolysosome formation is the last step in autophagy,

where LC3-II is cleaved from PE and recycled to the cytosol, and p62/SQSTM1 is degraded (105, 127). The degraded products, such as amino acids, lipids and sugars, are transferred back to the cytosol for reuse during starvation for macromolecule synthesis and/or to supply the cell with energy. Inhibition of the lysosomal H^+-ATPase using chemicals such as bafilomycin or chloroquine inhibits the fusion of autophagosomes with lysosomes (128), suggesting that the lysosomal function requires an acidic condition for proper fusion.

1.6 Signalling pathways regulating autophagy

1.6.1 mTOR pathway in regulation of autophagy

The mammalian target of rapamycin kinases (mTOR) are part of two complexes; the rapamycin-sensitive mTOR complex 1 (mTORC1) and mTOR complex 2 (mTORC2), which is not a direct regulator of autophagy. mTORC1 consists of a catalytic subunit, raptor, the G protein β-subunit-like protein (GβL), and proline-rich Akt substrate of 40 kDa (PRAS40). mTORC2 is composed of rictor, rapamycin-sensitive companion of mTOR, GβL, SAPK-interacting protein 1(SIN1), and protein observed with rictor (PROTOR) (129). Signals such as growth factors, amino acids, and glucose, and fatty acids regulate mTORC1. Under nutrient poor conditions, mTORC1 activity is suppressed and autophagy is induced. (98). On the other hand, nutrient availability leads to mTORC1 activation and autophagy suppression.

Rapamycin, a macrolide antibiotic isolated from *Streptomyces hygroscopicus*, inhibits mTOR activity (130), resulting in reduction of the phosphorylation of two downstream effectors of mTORC1, ribosomal protein S6 kinase-1 (S6K1) and translation

initiation factor 4E binding protein-1 (4E-BP1) at Thr389/Thr421/Ser424 and Thr37/Thr46, respectively (131). In mammalian cells, rapamycin forms a complex with immunophilin FK506-binding protein of 12 kDa (FKBP12) and stabilizes raptor-mTOR1, deactivating the kinase activity of mTOR, and inducing autophagy (132).

The ULKs-Atg13-FIP200 complex is a downstream target of mTORC1. Mammalian Atg13 associates with ULK1/ULK2, and mediates the interaction of ULK1/ULK2 with FIP200, forming a ULK1/2-Atg13-FIP200 complex. Under normal conditions, mTORC1 interacts with ULK1/2-Atg13-FIP200 complex, and inhibits the kinase activity of Atg13 and ULK1, hence suppressing autophagy (133). During starvation or rapamycin treatment, autophagy is induced through di ssociation of mTORC1 from the ULK1/2-Atg13-FIP200 complex, resulting in stimulation of ULK1 and ULK1-mediated phosphorylation of Atg13-FIP200, which then trigger autophagy (133).

1.6.2 PI3K regulation of mTOR and autophagy

Binding of insulin or growth factors to their receptors on the cell surface stimulates PI3K signaling, resulting in the conversion of phosphatidylinositol-4,5-bisphosphate to phosphatidylinositol-3,4,5-triphosphate (PIP3). PIP3 recruits the serine/ threonine kinases phosphoinositide-dependent kinase 1 (PDK1) and protein kinase B (Akt) to the plasma membrane, leading to phosphorylation of Akt by PDK1 (134). Activated Akt enhances phosphorylation of tumor suppressor proteins mutated in tuberous sclerosis (TSC2) a GTPase-activating protein for Ras homologue enriched in brain (rheb), which then inhibits formation of a TSC1/TSC2 complex by blocking the

interaction of TSC2 with TSC1. As a result the GTP-binding protein rheb is converted into the active GTP-bound form and stimulates the raptor-mTOR complex leading to suppression of autophagy (131, 134). PI3K classes have different roles in autophagy; the product of the class I PI3K (PIP_3) suppresses autophagy by activation of Akt, while the class III PI3K product (PI3P) activates autophagy (137).

1.6.3 Hypoxia

Tumors, cardiovascular ischemia, and brain injuries cause hypoxia activation of the transcription factor hypoxia-inducible factor-1 (HIF-1) (138). HIF-1 upregulates genes involved in erythropoiesis and angiogenesis, and decreases mitochondrial biogenesis. In mouse embryonic fibroblasts (MEFs), autophagy was dependent on HIF-1 and Bcl-2 adenovirus E1aa nineteen kDa interacting protein 3 (BNIP3). BNIP3 prevented beclin1 from interacting with Bcl-2, thereby inducing autophagy (139). However, a study in tumor cells found that activation of autophagy by hypoxia is independent on HIF-1, but relied on AMPK-mTOR signaling (140, 141). Hypoxia supresses mTOR and prevents translation of eukaryotic initiation factor4E (eIF-4F) complex, leading to autophagy induction. It seems that hypoxia can induce autophagy through either HIF-1-dependent or -independent pathways. Interestingly, in addition to upregulation of autophagy, hypoxia also stimulates PC biosynthesis by increasing CKα expression and phosphocholine synthesis within the hypoxic region (142).

1.6.4 ER stress

Stimulation of ER stress by glucose deprivation, oxidative stress, hypoxia and calcium release from the ER causes accumulation of unfolded protein in the ER, resulting in induction of autophagy (138). ER stress-induced autophagy is critical for cell viability through removal of the expanded and damaged ER resulting from unfolded protein response (UPR) (143). However, the mechanism of how ER stress induces autophagy depends on the stress condition and the organism.

In yeast, UPR signaling is mediated by inositol-requiring kinase 1 (IRE1), an ER transmembrane protein consisting of a cytosolic endoribonuclease domain and a lumenal stress-sensing domain. In response to an ER stress stimuli, the ER heat shock protein 70 (Grp78/Bip) dissociates from the IRE1 ER sensing domain, which activates the cytosolic endonuclease domain to process the mRNA for Hac1, a transcriptional activator. Hac1 transcriptionally activates genes involved in phospholipid biosynthesis, protein modification, and ER-associated degradation (ERAD). However, the function of IRE1-Hac1 pathway in activation of autophagy is still unclear (144).

In mammalian cells, silencing of Grp78/Bip supresses autophagosome formation triggered by either ER stress or starvation, without any effect on beclin1 or PI3K (145). These findings suggest that Grp78/Bip is essential for phagophore expansion after the induction step. As mentioned earlier, ER stress leads to increased intracellular calcium and promotes autophagosome accumulation. This process is mediated by calcium-activated calmodium-dependent kinase β (CaMKKβ) and AMP-activated protein kinase (146). In immortalized hepatocytes, the elevated level of calcium, induced by

thapsigargin and tunicamycin (ER stressors), leads to protein kinase C activation and promotes LC3-I lipidation (147).

1.7 Autophagy and cancer

The role of autophagy in cancer is controversial. On one hand, autophagy maintains normal cellular homeostasis through removal of cellular waste. On the other hand, autophagy supports cell survival during conditions such as hypoxia and starvation, which could facilitate the rise and growth of tumours

Some autophagy genes, such as Atg4, beclin1 and Atg5, have tumor suppressor activities. For instance, treatment of *Atg4-/-* mice with a carcinogen caused tumorigenesis in comparison with the wild type controls (148). p53, a tumor suppressor gene, trans-activates genes involved in autophagy induction, such as Damage Regulated Autophagy Modulator 1 (DRAM1) (149). Other evidence in favour of autophagy as a tumor suppressor comes from beclin1, which is mono-allelically deleted in a high percentage of human breast, ovarian and prostate cancers. These findings suggest that disruption of autophagy may be essential in tumorigenesis. Recently, a study found that autophagy prevents DNA-damage and chromosomal defects, especially in cells exposed to metabolic stress (150). This effect might be due to the role of autophagy in clearance of damaged proteins, thus preventing accumulation of reactive oxygen species (ROS). In another study, accumulation of p62/SQSTM1 in autophagy-deficient cells promoted DNA damage by ROS resulting in tumor formation (151). Therefore, suppressing autophagy causes genomic instability and cancer progression.

Other studies support the concept that autophagy promotes cancer cell growth and survival, arguing that cancer cells rely on autophagy to survive under conditions of nutrient deprivation and hypoxia. Inhibition of autophagy pharmacologically in colorectal cancer cell lines induces cell death (152). A recent study mentioned that the p53 levels appear to be decreased in many tumors, which causes induction of autophagy (153). Similarly, the activation of autophagy in p53 mutant cells might aid cancer cells to resist apoptosis (153). Similarly, following chemo-radiotherapy treatments, upregulation of autophagy is a protective mechanism to evade apoptosis (154). Altogether, autophagy has dual roles as a tumor suppressor and to maintain cancer cells survival in conditions of increased metabolic stress, hypoxia and cancer therapy.

1.8 Lipophagy and lipid mobilization

The liver converts fatty acids into triglyceride (TG) and stores it with cholesterol esters in lipid droplets (LD). During starvation, TG hydrolysis by lipases is upregulated to deliver fatty acids for energy production. Autophagy has a role in transferring lipids from LDs to be degraded by the lysosome through a process called lipophagy. Inhibition of autophagy either pharmacologically or genetically increased the number and size of LDs in hepatocytes in the presence of oleic acid. In addition, electron microscopic study found increased co-localization of neutral lipids with autophagosomal (LC3-II) and lysosomal proteins (LAMP1) when autophagy is activated (155).

Autophagy has also been implicated in regulation of liver diseases such as non-alcoholic and alcoholic steatohepatitis, where excess fatty acids are stored in LDs as TG. Studies have demonstrated that alcohol induces macroautophagy to prevent accumulation

of LD and protect against ethanol-induced toxicity in liver, such as development of steatohepatitis (156). Similarly, the number of autophagosomes was increased in the liver of alcohol-fed animals contained LDs. Altogether, lipophagy is a new player in LD degradation and could be considered as an energy-making pathway (156).

1.9 Crosstalk between phospholipids and autophagy

Lipids regulate autophagosome formation either as a component of the double-membrane or as signalling molecules. VPS34 phosphorylates PI to PI3P and is required in phagophore formation (157). After induction of autophagy, the phagophore is formed from a specific phosphatidylinositol 3-phosphate (PI3P) enriched membrane structure called omegasome in mammals and PAS in yeast (158). The omegasome is derived from the ER. PI3P plays a role during phagophore elongation through the PROPPIN family or WD repeat domain phosphoinositide-interacting (WIPI) proteins, which belong to a family of PI3P effector proteins. Three PROPPINs, WIPI-1, WIPI-2, and WIPI-4 are involved in autophagy initiation in mammals (159). WIPI-1 and WIPI-2 bind to PI3P-enriched phagophores, which then facilitate the recruitment of the ATG5-ATG12-ATG16L1 complex and aid the conjugation of LC3 with PE, the two complexes required for phagophore elongation (160, 161). Deletion of WIPI-2 in HEK293A cells caused an accumulation of omegasome and a defect in LC3 lipidation (162), meaning that WIPI-2 is necessary for autophagosome formation. The autophagy-linked FYVE protein (Alfy) is a PI3P binding protein, which is involved in degradation of protein aggregates during autophagy activation (163). Alfy binds with multiple autophagic components such as

p62/SQSTM1, ATG5 and PI3P via its FYVE domain, acting as a scaffold protein to recruit and targeting protein aggregates to autophagosomes for degradation (164).

The balance between PI3P production by Vps34 and breakdown by PI3P phosphatases is essential for the autophagosome closure, maturation and fusion with the lysosome (165). PI3P phosphatases of the myotubularin (MTMR) family, such as MTMR14 (Jumpy) dephosphorylate PI3P and negatively regulate autophagy by controlling the recruitment of WIPI-1 (166). Inhibition of Jumpy using a small molecule called AUTEN-67 increases autophagic flux in Hela cells (167). A study identified the PI3P effector protein Tectonin domain-containing protein 1 (TECRPR1) in autolysosome formation (168). TECRPR1 binds with the ATG5-ATG12 complex and PI3P to facilitate autophagosome–lysosome fusion. Deletion of TECRPR1 prevents fusion of autophagosomes with the lysosome and inhibits autophagic degradation of p62/SQSTM1 and LC3-II (168). Taken together, PI3P is a key player for autophagy regulation either directly or through recruitment of specific autophagic effectors.

PE is the main lipid required for phagophore expansion to engulf the cargo for degradation. LC3 is diffuse in the cytoplasm under normal condition, but during starvation, it fuses with PE to form a complex to bind to the autophagic membranes until the degradation, where LC3 dissociate from PE. However, whether PE metabolism directly impacts autophagy has not been tested.

PA produced by hydrolysis of PC by PLD constitutes 1-4% of total cellular lipids (169). PA regulates several stages of autophagy. For instance, PA interacts with the domain of mTOR targeted by rapamycin hence activating mTOR and suppressing autophagy (170). In addition, blockage of PC hydrolysis by inhibition of PLD1

suppresses the interaction of beclin1 with the Vps34 complex, resulting in autophagy suppression (171). In that study, PLD1 inhibition significantly sensitized *in vivo* cancer regression through genetic and pharmacological suppression of autophagy.

Another study found a different role for endo-lysosomal PLD1 in autophagy (172). During starvation, PLD1 activity was induced on the outer membrane of autophagosomes. (172). Inhibition of PLD1 pharmacologically or by genetically deletion in CHO cells and MEFs, respectively, decreased the production of LC3-positive structure, hence inhibiting autophagosome formation (172). These results suggest that the hydrolysis of PC by PLD1 is involved in autophagosome formation.

These data provide evidence that phospholipids are involved in autophagy regulation. The synthesis of most phospholipids occurs at the ER, where the phagophore originates, provides strong evidence that synthesis of phospholipids is necessary for the autophagosome biogenesis. However, the involvement of PC in autophagosome formation has not been investigated even though it constitutes that majority of lipids in that structure.

1.10 Aims for this study

A hallmark of cancer is increased lipogenesis, including PC biosynthesis to enable sustained cell proliferation and membranes synthesis (173). Oncogenic ras, which is mutated in more than 30% of human cancer, promotes overexpression and/or activation enzymes of the CDP-choline pathway, such as CKα and CCTα to provide PC needed for membrane synthesis during proliferation, evasion of apoptosis and anchorage-dependent cell death (anoikis) (73, 174). Recently, our lab found that disruption of PC biosynthesis by knocking down CCTα sensitized ras-transformed cells (IEC-ras) to anoikis (39). Previous studies have shown that autophagy is upregulated in ras-transformed cells, and its inhibition drives the cells to apoptosis (175, 176). Since the site of autophagy initiation and PC biosynthesis takes place at the ER, the increase of PC biosynthesis in IEC-ras cells could be to promote autophagy. I hypothesize that since the final step of PC biosynthesis also takes place at the ER, PC synthesis is directly involved in autophagosome double membrane formation. My project was divided into two aims to address how PC biosynthesis by the CDP-choline pathway contributes to the survival of IEC-ras-transformed cells:

1) Does elevated CCTα expression promote survival and anoikis-resistance of ras-transformed cells by an autophagy-related mechanism?
2) Does disruption of PC biosynthesis by choline depletion affect autophagy and proliferation of ras-transformed cells?

CHAPTER 2 MATERIALS AND METHODS

2.1 Materials

A mouse anti-β-actin monoclonal antibody, bovine serum albumin (BSA), polybrene, lentiviral shCCTα pLKO.1 plasmids, non-targeting shRNA (shNT), chloroquine diphosphate salt and Choline chloride, were purchased from Sigma-Aldrich (St. Louis, MO). Plasmid purification kits were purchased from Qiagen (Missisauga, ON). Mowiol 4-88 was purchased from EMD Biosciences (La Jolla, CA). Sea Plaque agarose was purchased from Cambrex (Rockland, ME). Alexa-Flour 488-conjugated-goat anti-rabbit antibody, Dulbecco's modified Eagle's medium (DMEM), ampicillin, carbenicillin, kanamycin, puromycin were purchased from Invitrogen (Burlington, ON). An antibody against the C-terminus of CCTα was raised in rabbits, purified, and purchased from Genscript (Scotch Plains, NJ). A rabbit polyclonal anti-beclin1 antibody was purchased from Santa Cruz Biotechnology. A P62/SQSTM1 antibody was purchased from Abcam (Toronto, ON). Antibodies to detect PARP1, ATG5 and ATG7 were purchased from Cell Signaling Technology (Danvers, MA). An LC3 antibody was purchased from Novus Biologicals (Oakville, ON). Odyssey blocking buffer was purchased from LI-COR Biosciences (Lincoln, NE). Nitrocellulose (NC) membrane, TEMED, glycine, 40% acrylamide, and Tween-20 were purchased from Bio-Rad (Hercules, CA). Polyethyleneimine (PEI) was purchased from Polysciences (Warrington, PA). Lyso-PC was purchased from Avanti Polar Lipid, Inc (Alabaster, AL).

2.2 Cell culture

All cells used in this study were cultured at 37ºC in a humidified 5% CO_2 atmosphere. Non-malignant rat IEC-18 and transformed IEC-ras clones (IEC-ras34, IEC-ras33, and IEC-ras37) were cultured in α-minimal essential medium (MEM) containing 5% fetal bovine serum (FBS), D-glucose (3.6 g/L), insulin (12.7 μg/mL), penicillin (600 μg/mL), streptomycin (100 μg/mL) and glutamine (2.9 mg/mL) (IEC-MEM). HEK293T cells were cultured in Dulbecco minimal essential medium containing 10% FBS (DMEM-FBS). For choline depletion experiments, IEC and IEC-ras were grown in choline-free DMEM with 5% FBS (CF-DMEM).

2.3 Lentiviral silencing of CCTα

Knockdown of CCTα was performed using the following shCCT3 sequence CCGGCCTGTGAGAGTTTATGCGGATCTCGAGATCCGCATAAACTCTCACAGG TTTTTG, and non-target shNT CCGGCAACAAGATGAAGAGCACCAACTCGAGTT GGTGCTCTTCATCTTGTTG TTTTT. These shRNAs were previously validated (39).

A lentiviral delivery system was used to silence CCTα. Lentivirus was produced by co-transfection of plasmids encoding envelope protein vesicular stomatitis virus glycoprotein (VSVG), packaging factors (Δ 8.2) and a pLKO.1 vector encoding an CCTα or non-targeting shRNA into HEK293T cells. Six μg of pLKO.1-shRNA, 6 μg of Δ8.2 plasmid, 1 μg of L-VSVG plasmid and 40 μL polyethyleneimine (PEI) transfection reagent were added to 800 μL of DMEM. The mixture was vortexed for 5 sec, incubated at room temperature for 15 min, added to 6 mL of HEK293T cells (8×10^6) in DMEM-

FBS, cultured on 100 mm dishes and cells were allowed to produce viral particles for 48 h. Virus-containing media was harvested, passed through a 0.45 um filter and 1 μg/mL of Polybrene, a cationic polymer, was added to aid viral entry into the cell. Three ml of the virus-containing media was diluted up to 5 ml by adding 2 ml of serum-free DMEM, applied to a culture of 70% confluent IEC-18 or IEC-ras34 cells for 4 h and 8 ml of IEC-MEM was added. After 24 h, fresh IEC-MEM containing 1 μg/ml and 5 μg/ml puromycin was added to IEC-18 and IEC-ras34 cells, respectively, for 48 h to kill non-infected cells. The efficiency of CCTα knockdown was determined by immunoblotting.

2. 4 Immunoblotting

Cells were rinsed once with cold phosphate-buffer saline (PBS), and prepared in SDS-PAGE buffer (12.5% SDS, 30mM Tris-HCl (pH 6.8), 12.5% glycerol, and 0.01% bromophenol blue). Cell lysates were then sonicated at 60 Hz for 20 s and heated to 90 °C for 5 min. Samples were separated by SDS-PAGE using SDS-running buffer (3 mM SDS, 200 mM glycine and 25 mM Tris-base) for 1 h at 120 V. Proteins were transferred to nitrocellulose membrane using transfer buffer (25 mM Tris-base, 192 mM glycine, 20% methanol) for 1 h at 100 V. Protein transfer was confirmed by Ponceau staining (0.1% Ponceau-S, 30% trichloroacetic acid, 5% sulfosalicylic acid). The membranes were incubated in Odyssey blocking buffer-TTBS (20 mM Tris-HCl, [pH 7.4] 500 mM NaCl, 0.05% Tween 20); 1:5, v/v). Primary antibodies were diluted in blocking buffer at specific concentration, [actin (1:10000), p62/SQSTM1, LC3, ATG5, ATG7, beclin1, PARP1 (1:1000), CCTα (1:2000)] incubated for 1 h at room temperature (ATG5- ATG7 antibodies were incubated overnight at 4°C), followed by secondary antibodies at

1:15000 dilutions in blocking buffer for 1 hr. Fluorescence was detected at 680 nm or 800 nm using the Odyssey infrared imaging system, and quantified using Odyssey Application Software v3.0. All proteins were quantified relative to an actin load control.

2.5 Choline depletion of cultured cells

IEC-18 and IEC-ras (100,000 cells) were seeded on 60 mm dishes in IEC-MEM, and cultured for 24 h prior to starting the experiment. Media were changed to CF-DMEM with 5% FBS. Cells were grown for 3, 6, 12, 24 and 48 h, washed with cold PBS, harvested and lysed with SDS-PAGE buffer and probed with antibodies (see figure legends). Protein expressions in choline-depleted cell were compared with cells cultured in the same media containing 40 μM choline.

2.6 Rescue of choline-depleted cells with lyso-PC

This experiment was done to investigate whether lyso-PC could restore autophagy in choline-depleted IEC-ras34 cells. Cells (100,000) were plated on 60 mm dishes in IEC-MEM, and cultured for 24 h prior to starting the experiment. Media were then replaced with fresh IEC-MEM (control), CF-DMEM and CF-DMEM supplemented with 50 μM of lyso-PC dissolved in ethanol and CF-DMEM supplemented with 40 μM of choline dissolved in water. Cells were cultured for 24 h, washed with cold PBS, harvested and lysed in SDS-page buffer and probed with antibodies (see figure legends).

2.8 Autophagic flux monitoring using chloroquine

Cells (100,000) were plated on 60 mm dishes in IEC-MEM, and cultured for 24 h prior to starting the experiment. Media were then replaced with fresh IEC-MEM and CF-DMEM. Cells were grown for 20 h and then cells were treated with or without chloroquine (400 μm, stocks prepared in water) for 4 h, washed with cold PBS, lysed with SDS-page buffer and probed with antibodies (see figure legends).

2.9 Clonogenicity assay for cell viability

IEC-18 and IEC-ras34 (500 cells) were seeded onto 60 mm dishes coated with 2 mL of 1% (w/v) Sea Plaque agarose (SP-agarose) in IEC-MEM, (SP-agarose was diluted in CF-DMEM+/- choline for control and choline-depleted cells, respectively). Cells were diluted with CF-DMEM+/- 40 μm of choline to up to 2 ml. An adherent control consisted of 500 seeded directly onto 60 mm dishes without SP-agarose. Cells on SP-agarose were transferred to dishes after 12, 24, 48 h and cultured in IEC-MEM for 72 h (SP-agarose was washed with 2 mL IEC-MEM to ensure all cells were completely transferred). After 4 days, colonies were washed with PBS, fixed with methanol:acetic acid (2:1 v/v) and stained with crystal violet. Colonies were counted and survival determined relative to the adherent control.

2.10 Immunofluorescence microscopy

Cells cultured on sterile glass cover slips (0.15 mm) were washed with cold PBS (10 mM Na_2HPO_4 [pH 7.4], 137 mM NaCl, 2.7 mM KCl and 2 mM KH_2PO_4), fixed with 4%

paraformaldehyde (w/v) for 15 min at room temperature. Cells were washed with 50 mM ammonium chloride to quench any paraformaldehyde, permeabilized using 0.5 % Triton X-100 for 10 min at 4 ºC. After permeabilization, coverslips were incubated in PBS containing 1% (w/v) BSA (PBS/BSA) for 1 h at room temperature. Primary antibodies were diluted in PBS/BSA at specific concentrations, incubated for 1 h at room temperature. The coverslips were washed twice with PBS/BSA for 5 min each. Secondary antibodies were diluted at 1:5000 in PBS/BSA, incubated for 1 h at room temperature. The coverslips were washed twice with PBS/BSA for 5 min each and the last wash with distilled water. The coverslips were then mounted on glass slides with 15 µL Mowiol for 1 h, and images were captured using either a Zeiss Axiovert 300M fluorescent microscope equipped with an AxioCamHR camera and a 100x oil-objective lens, or Zeiss LSM 510 upright laser scanning confocal microscope using 63x oil immersion lens and ZEN 2009 software. Confocal sections were typically 0.6 µm thickness.

2.11 Measuring cell proliferation

IEC-18 and IEC-ras34 (10,000 cells) were seeded on 35 mm dishes in IEC-MEM, and cultured for 24 h prior to starting the experiment. Media were changed to CF-DMEM +/- 40 µm of choline. Cells were grown for 12, 24 and 48 h, washed with PBS, trypsinized and counted using a haemocytometer.

2.12 Statistical analysis

Statistical analysis of data shown was performed using Students two-tailed t-test. Error bars represent the standard error of mean (SEM). The significance is marked for $p < 0.05$ (**), and $p < 0.01$ (***).

CHAPTER 3 RESULTS

3.1 The role of CCTα in autophagy regulation in IEC-ras transformed cells.

The detachment of normal intestinal epithelial cells (IEC) from the extracellular matrix (ECM) induces anoikis through an integrin-dependent mechanism (81). IEC-ras33, IEC-ras34, IEC-ras37, were generated by transfection of IEC-18 with a mutant H-ras oncogene cloned from human bladder carcinoma (177). These IEC-ras clones grow in three-dimensional culture (detached from the ECM) through activation by H-Ras pathways that promote apoptosis suppression and survival (178). CCTα expression was increased in IEC after transformation with mutant ras oncogene (30-fold in IEC-ras33, 10-fold in IEC-ras34 and 15-fold in IEC-ras37) compared to normal IEC-18 (39). IEC-18 loss PC biosynthesis rapidly after detachment from the ECM and undergo anoikis, (39). On the other hand, IEC-ras cells had increased PC synthesis and decreased PC breakdown compared to adherent cells, indicating that the PC biosynthesis is linked to anoikis resistance. In support of this conclusion, knockdown of CCTα using shRNA induced anoikis in IEC-ras34 (39). Thus, ras oncogene increased CCTα expression and PC biosynthesis is required for building membranes to compensate the high proliferation rate of transformed cells, promoting cell survival and anoikis resistance.

This study investigated whether CCTα and PC biosynthesis play a role in anoikis resistance of IEC-ras through an autophagy-related pathway. First, I checked whether ras oncogene affects the expression of ATG5 and ATG7 in IEC-ras34 compared to IEC-18. ATG5 and ATG 7 are implicated in phagophore elongation where ATG5 forms a

complex with ATG12 while ATG7 aids in LC3 lipidation as well as ATG5-ATG12 complex formation (98). The expression of ATG5 and ATG7 was determined by immunoblotting in total cell lysates of IEC-18 and IEC-ras34 cultured under adherent conditions. The expression of ATG5 and ATG7 were increased in IEC-ras34 with 5.7-fold and 5.4-fold, respectively, compared to IEC-18 (**Fig 3. 1. 1).** This result indicates that autophagy could be increased in IEC-ras34 cells and that overexpression of CCTα and ATG proteins in IEC-ras34 might be interrelated.

Next, I investigated the role of CCTα in autophagy in adherent and detached IEC-18 and IEC-ras34. First, CCTα was knocked down in IEC-18 and IEC-ras34 by lentiviral expression and puromycin selection of cells expressing a short hairpin RNA (shRNA). The knockdown efficiency of CCTα was confirmed using immunoblotting (**Fig. 3. 1. 2**), which indicated an efficiency of about 95% compared to cells transduced with a non-targeting shRNA.

After knocking down CCTα, IEC-18 were cultured under detached conditions on SP-agarose for up to 12 h while IEC-ras34 were cultured for up to 72 h. The difference in time points between IEC-18 and IEC-ras34 is because IEC-18 die after 24 h of detachment and IEC-ras34 can survive for 72 h. Previous studies have shown that detachment of non-malignant intestinal epithelial cells from ECM induced autophagosome formation and protected cells from anoikis (179-181). Autophagy was investigated using immunoblotting to examine LC3 and p62/SQSTM1 expression, which are commonly used markers of autophagy. Under attached conditions for IEC-18 expressing

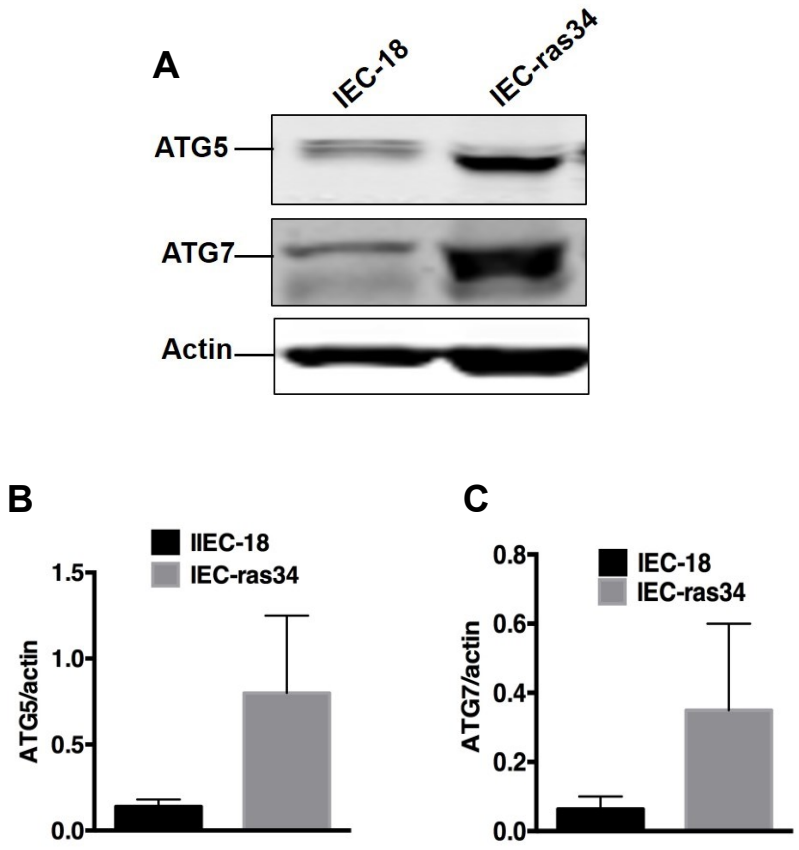

Figure 3.1.1: ATG5 and ATG7 expression in IEC-18 and IEC-ras34. IEC-18 and IEC-ras34 were cultured in the presence of choline. Total cell lysates were separated by SDS-PAGE and immunoblotted for ATG5, ATG7 and actin (**A**). Immunoblots were visualized with Odyssey infrared imaging system. The relative ratio of ATG5 (**B**) and ATG7 (**C**) was measured compared to actin. Results are the mean and range of two independent experiments.

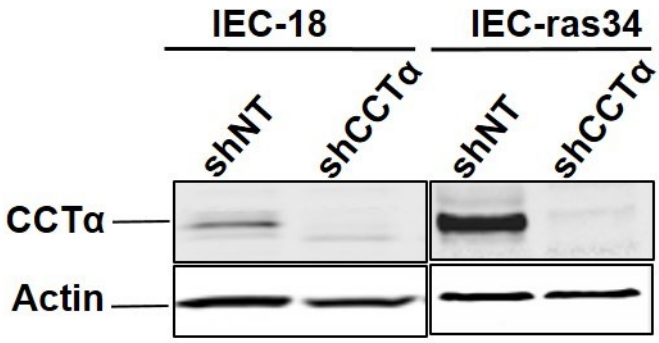

Figure 3.1.2: CCTα expression in IEC-18 and IEC-ras34 was knocked down using lentivirus encoding shCCTα. IEC-18 and IEC-ras34 were transduced with lentivirus encoding shRNA against CCTα or non-targeting shRNA and selected with puromycin for 48 h. Cells were then harvested and total cell lysates were separated by SDS-PAGE, immunoblotted for CCTα and actin. Immunoblots were visualized with Odyssey infrared imaging system.

shNT (IEC-shNT), both p62/SQSTM1 and LC3-II were low (**Figure 3.1.3. A**) and detachment of IEC-shNT caused a slight increase in LC3-II, especially after 12 h of detachment, and a remarkable increase in p62/SQSTM1 levels started after a 3 h of detachment. In attached IEC-18 CCTα knockdown cells (IEC-shCCTα), expression of both LC3-II and p62/SQSTM1 was low, similar to the IEC-shNT. During detachment, p62/SQSTM1 accumulated, especially after 12 h, to a level similar to shNT cells (**Figure 3.1.3. A**).

Whether CCTα knockdown affected autophagy in adherent and detached IEC-ras34 was also tested. Similar to IEC-18, LC3 and p62/SQSTM1 were investigated by immunoblotting (**Figure 3.1.3.B**). In IEC-ras34 expressing shNT (IEC-ras-shNT), the level of LC3-II was high when cells were attached but decreased at 12 h after detachment and then started to increase again at 48. In addition, the degradation of p62/SQSTM1 was increased with time under detached conditions. In adherent IEC-ras34 expressing shCCTα (IEC-ras-shCCTα), LC3-II and p62/SQSTM1 levels were 1.3 and 3.6-fold higher respectively, than in adherent shNT cells. Upon detachment of IEC-ras-shCCTα, p62/SQSTM1 significantly increased by 4-fold after 48 and 72 h of detachment compared to IEC-ras-shNT. Immunofluorescence experiment also showed accumulation of p62/SQSTM1 puncta in IEC-ras-shCCTα compared to non-targeted cells (**Figure 3.1.4).** The p62/SQSTM1 accumulation in adherent and detached IEC-ras34 CCTα knockdown cells indicates a defect in autophagy.

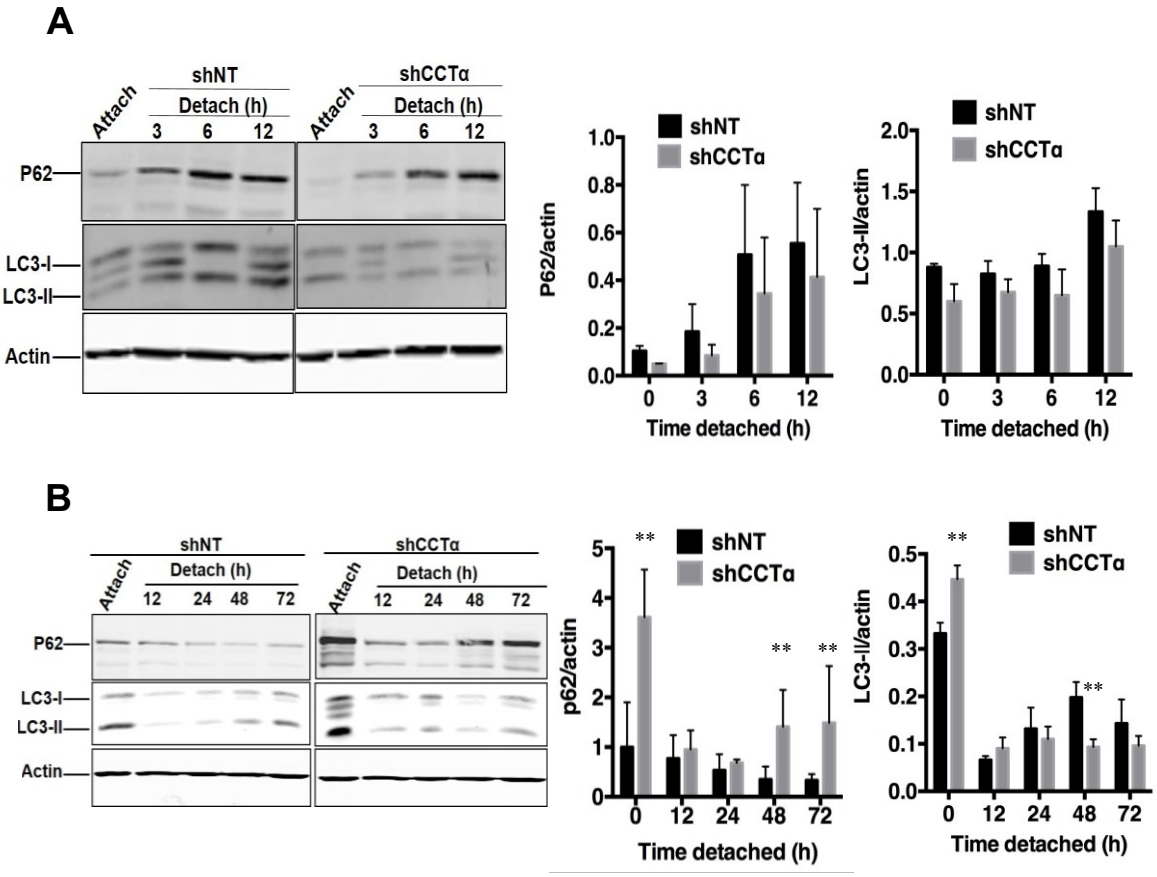

Figure 3.1.3: Effect of CCTα knockdown on autophagic markers in adherent and detached IEC-18 and IEC-ras34. IEC-18 and IEC-ras34 were infected with lentivirus encoding shRNA against CCTα or non-targeting control (shNT) and selected with puromycin for 48 h. Cells were cultured on SP-agarose for the indicated times, harvested, lysed in SDS-PAGE buffer, separated by SDS-PAGE, immunoblotted for p62/SQSTM, LC3 and actin. Immunoblots of IEC-18 (**A**) and IEC-ras34 (**B**) were visualized with Odyssey infrared imaging system. Results are the mean and range of two (**A**) and mean an SEM of three (**B**) independent experiments. ** $p < 0.05$ and *** $p < 0.01$ compared with shNT cells for each time point.

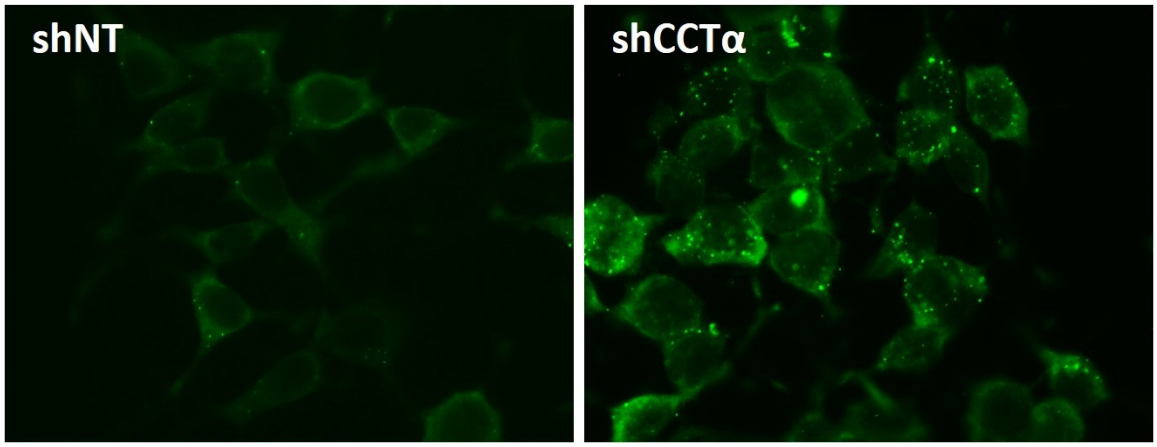

Figure 3.1.4: p62/SQSTM1 accumulated in adherent IEC-ras34 shCCTα knockdown cells. IEC-ras34 (shNT and shCCTα) cells were plated on coverslips, fixed, permeabilized and incubated overnight with rabbit anti-p62/SQSTM1 antibodies, followed by AlexaFluor488-conjugated goat anti-rabbit, and mounted on glass slides. Images were captured using a Zeiss Axiovert 300M fluorescent microscope equipped with an AxioCamHR camera and a 100x oil-objective lens (see section 2.10).

To further test the effect of CCTα silencing on autophagy, beclin1 was investigated using immunoblotting to determine whether a defect in autophagy occurred at an early stage. In adherent IEC-shNT cells, full-length (F) beclin1 was cleaved (C) to give a 40 kD product. However, detachment of IEC-shNT from dishes rapidly suppressed cleavage of beclin1 after 3 h. Similarly, IEC-shCCTα cells had the same phenotype with slightly more cleaved beclin1 relative to the full-length compared to IEC-shNT (**Figure 3.1.5.A**). In contrast, beclin1 in adherent IEC-ras-shNT cells was exclusively full-length. However, detachment of IEC-ras-shNT cells induced beclin1 cleavage after 48 h (**Figure 3.1.5.B**). CCTα knockdown in IEC-ras34 triggered cleavage of beclin1 in adherent cells compared to shNT cells. Similarly, detached IEC-ras-shCCTα cells had a significant increase in cleaved beclin1, especialy after 24 h of detachment, compared to the shNT cells, indicating autophagy deactivation (**Figure 3.1.5.B**).

Autophagy induction is critical for cancer cells survival and apoptosis resistance. A number of studies showed that inactivation of autophagy induced apoptosis and anoikis (179, 182). In this study, poly (ADP-ribose) polymerase-1 (PARP1) antibody was used to assess whether CCTα knockdown in IEC-18 and IEC-ras34 cells triggered apoptosis under adherent and detached conditions. Full-length 120 kD PARP1 is cleaved during apoptosis to a 89 kD fragment (183). In this study, detachment of IEC-shNT triggered PARP1 cleavage after 3 h (**Figure 3.1.6.A**). PARP1 was also cleaved in IEC-shCCTα after detachment (**Figure 3.1.6.A**), meaning that cleavage of PARP1 is not CCTα dependent. IEC-ras-shCCTα cells had 2-3 fold more PARP1 cleavage after detachment compared to IEC-ras-shNT cells (**Figure 3.1.6.B**). These data indicate that knocking down CCTα in IEC-ras34 cells triggered PARP1 cleavage.

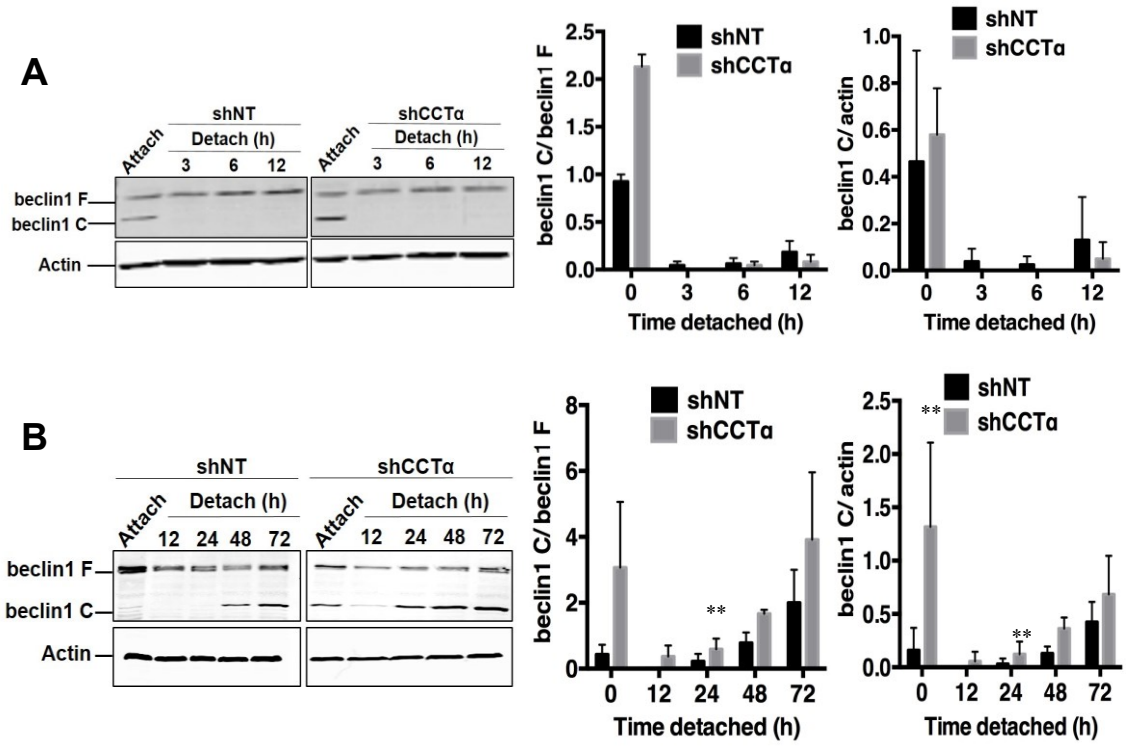

Figure 3.1.5: Effect of CCTα Knockdown on beclin1 in adherent and detached IEC-18 and IEC-ras34. IEC-18 (**A**) and IEC-ras34 (**B**) were infected with lentivirus encoding shRNA against CCTα or non-targeting control (shNT), selected with puromycin for 48 h. Cells were cultured on SP-agarose for the indicated times, harvested, lysed in SDS-PAGE buffer, separated by SDS-PAGE, immunoblotted for beclin1 antibody that detects beclin1 full length (beclin1 F) and the cleavage fragment (beclin1 C) and actin. Immunoblots of IEC-18 (**A**) and IEC-ras34 (**B**) were visualized with Odyssey infrared imaging system. Results are the mean and range of two (**A**) or the mean and SEM of three (**B**) independent experiments. ** $p < 0.05$ and *** $p < 0.01$ compared with non-target cells for each time point.

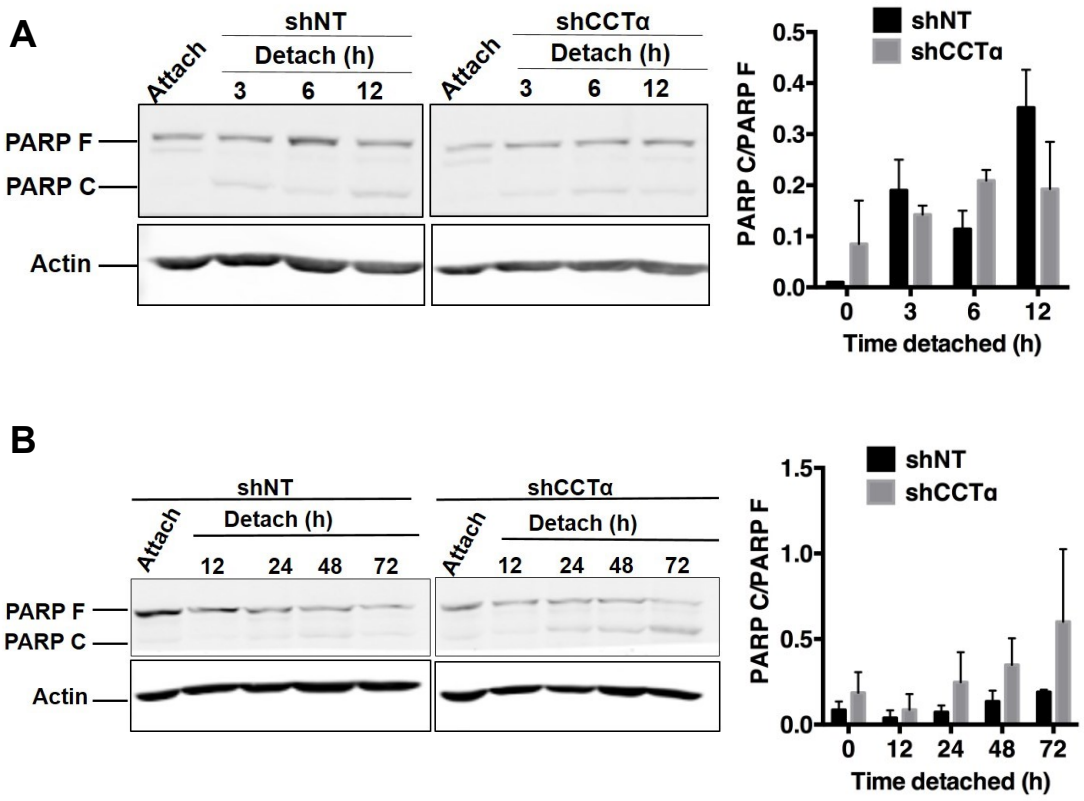

Figure 3.1.6: Effect of CCTα knockdown on PARP1 in adherent and detached IEC-18 and IEC-ras34. IEC-18 and IEC-ras34 were infected with lentivirus encoding shRNA against CCTα or non-targeting control (shNT). Cells were cultured on SP-agarose for the indicated times, harvested, lysed in SDS-PAGE buffer, separated by SDS-PAGE, immunoblotted for full-length (PARP1 F) and cleaved PARP1 (PARP1 C) and actin. Immunoblots of IEC-18 (**A**) and IEC-ras34 (**B**) were visualized with Odyssey infrared imaging system. Results are the mean and range of two independent experiments.

3.2 The effect of choline depletion on autophagy in normal IEC-18 and malignant IEC-ras34.

In the second part of this study choline depletion of cells was used as a model to decrease the synthesis of PC while CCTα was active. IEC-ras cells do not have PEMT, therefore exogenous choline in the media is the only source for making PC. Thus, we can test whether reduction of PC biosynthesis by choline depletion affects autophagy in IEC-18 and IEC-ras34 cells. To test this hypothesis, I first looked at the effect of choline depletion on ATG5 and ATG7 expression in IEC-ras34 cells. From western blotting, it is apparent that culturing cells in choline-free DMEM (CF-DMEM) did not affect ATG5 and ATG7 expressions (**Figure 3.2.1**).

Next, I investigated whether choline depletion affects autophagic in IEC-18 and IEC-ras clones. In this experiment, cells were cultured in the presence or absence of choline for up to 48 h then immunoblotting was used to check the expression of LC3 and p62/SQSTM1. In normal IEC-18 cells, depletion of choline from media did not affect LC3 and p62/SQSTM1 expression, suggesting autophagy was unaffected (**Figure 3.2.2.A**).

In IEC-ras34 cells, choline depletion caused a significant accumulation of p62/SQSTM1 after 24 h in comparison with cells cultured in presence of choline (**Figure 3.2.2.A).** LC3-II was also increased significantly in IEC-ras34 that were choline depleted for 24 h. Immunofluorescence experiment was also used to detect the p62/SQSTM1 punctate in IEC-18 and IEC-ras34 cells cultured in the presence and absence of choline for 24 h.

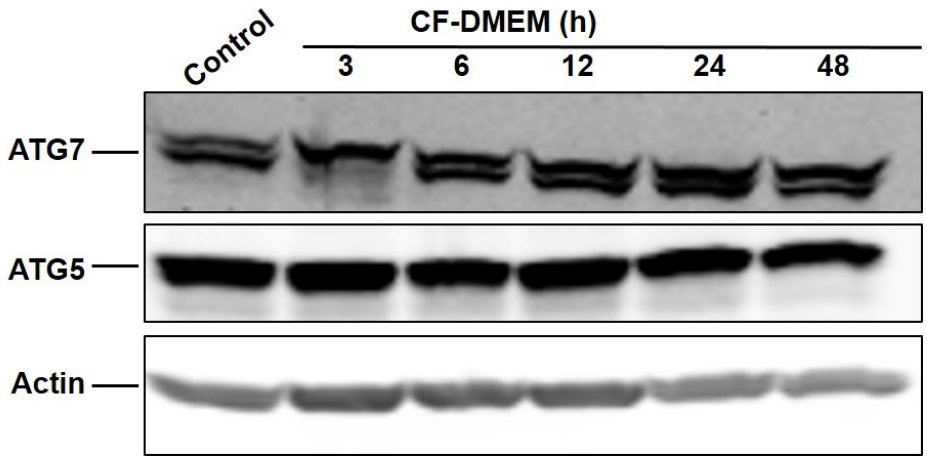

Figure 3.2.1: Effect of choline depletion on ATG5 and ATG7 expression in adherent IEC-ras34. IEC-ras34 cells were cultured in the presence or absence of choline for the indicated times. Cells were then harvested, lysed in SDS-PAGE buffer,separated by SDS-PAGE, immunoblotted for ATG5, ATG7 and actin. Immunoblots were visualized by Odyssey infrared imaging system. Control (cells cultured in 40 μM choline for 48 h)

Consistent with immunoblotting results, choline depletion of IEC-18 had no effect on p62/SQSTM1 punctate compared with IEC-18 cultured in the absence of choline for up to 48 h (**Figure 3.2.3**). In contrast, depletion of choline from media caused p62/SQSTM1 accumulation in IEC-ras34 at 12 h and increased for up to 48 h (**Figure 3.2.3**). Other IEC-ras clones (IEC-ras33 and IEC-ras37) were also examined to determine whether they exhibited the same phenotype as IEC-ras34. Choline depletion induced p62/SQSTM1 accumulation in IEC-ras33 and IEC-ras37 compared with control (**Figure 3.2.4**). LC3-II was also increased in choline-depleted IEC-ras33 but did not change in IEC-ras37. The p62/SQSTM1 accumulation and increased LC3-II levels in IEC-ras choline-depleted cells indicate an impairment of autophagy.

To test whether choline depletion caused accumulation of p62/SQSTM1 and LC3-II due to increasing autophagic flux or suppressing autophagy, IEC-ras34 cells were cultured in the presence or absence of choline for 20 h and then Chloroquine (CQ) was added for 4 h. CQ blocks autophagy at the fusion of autophagosome with lysosomes by increasing lysosomal pH (175). If the accumulation of P62/SQSTM1 and LC3 was due to an increase in autophagic flux, addition of CQ would synergize p62/SQSTM1 accumulation in choline-depleted cells. But if it was due to suppression of autophagy at or prior to

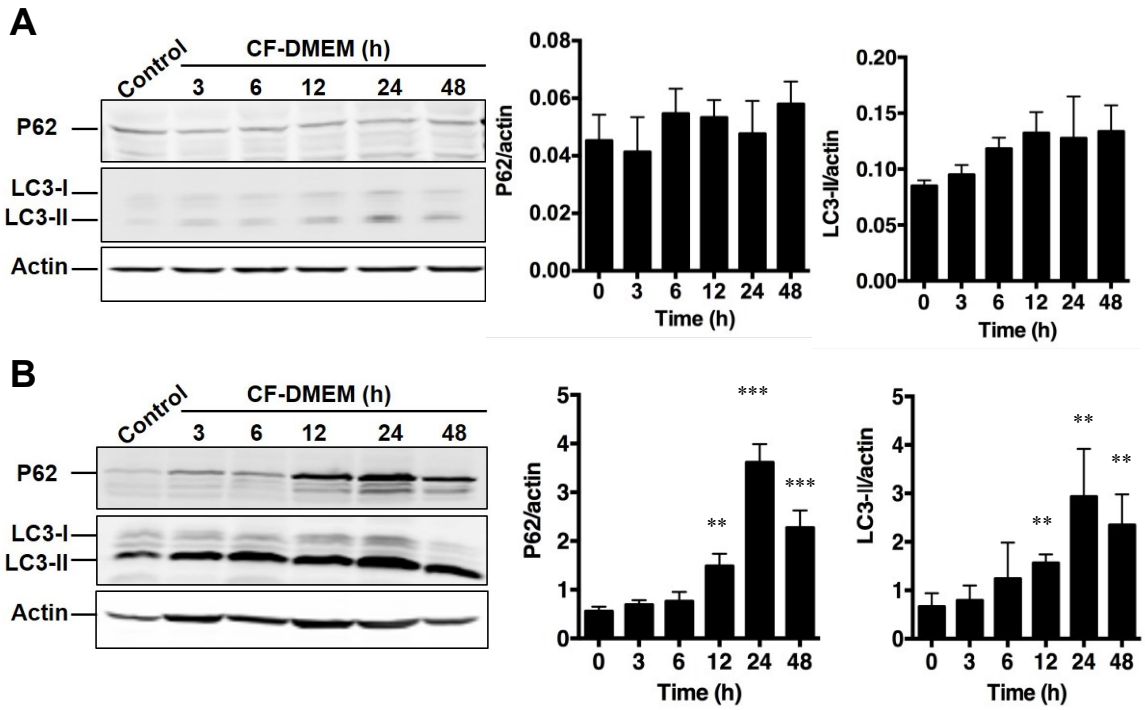

Figure 3.2.2: Effect of choline depletion on autophagic markers in adherent IEC-18 and IEC-ras34. IEC-18 and IEC-ras34 were grown in presence or absence of choline for the indicated times. Cells were then harvested, lysed in SDS-PAGE buffer, separated by SDS-PAGE, immunoblotted for p62/SQSTM1, LC3 and actin. Immunoblots of IEC-18 (**A**) and IEC-ras34 (**B**) were visualized by Odyssey infrared imaging system. Results are the mean and range of two (**A**) or the mean and SEM of three (**B**) independent experiments. ** $p < 0.05$ and ***$p < 0.01$ compared with control (cells cultured in 40 μM choline for 48 h).

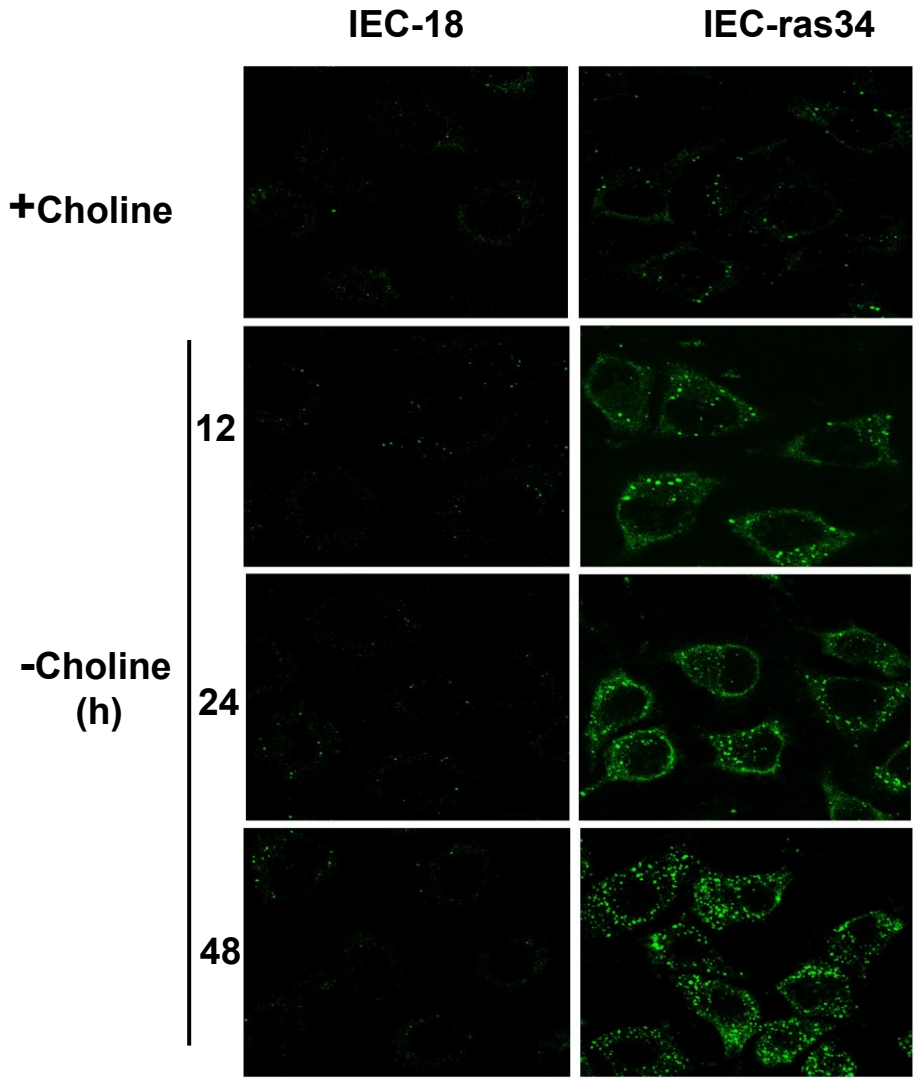

Figure 3.2.3: p62/SQSTM1 puncta accumulated in choline-depleted IEC-ras34. IEC-18 and IEC-ras34 were cultured on glass coverslips in the absence of choline for up to 48 h. Controls received 40 µM choline for 48 h. Cells were then fixed, permeabilized and incubated overnight with rabbit anti-p62/SQSTM1 antibodies, followed by AlexaFluor488-conjugated goat anti-rabbit, and mounted on glass slides. Images were captured using a Zeiss LSM 510 upright laser scanning confocal microscope using 63x oil immersion lens and ZEN 2009 software (see section 2.10).

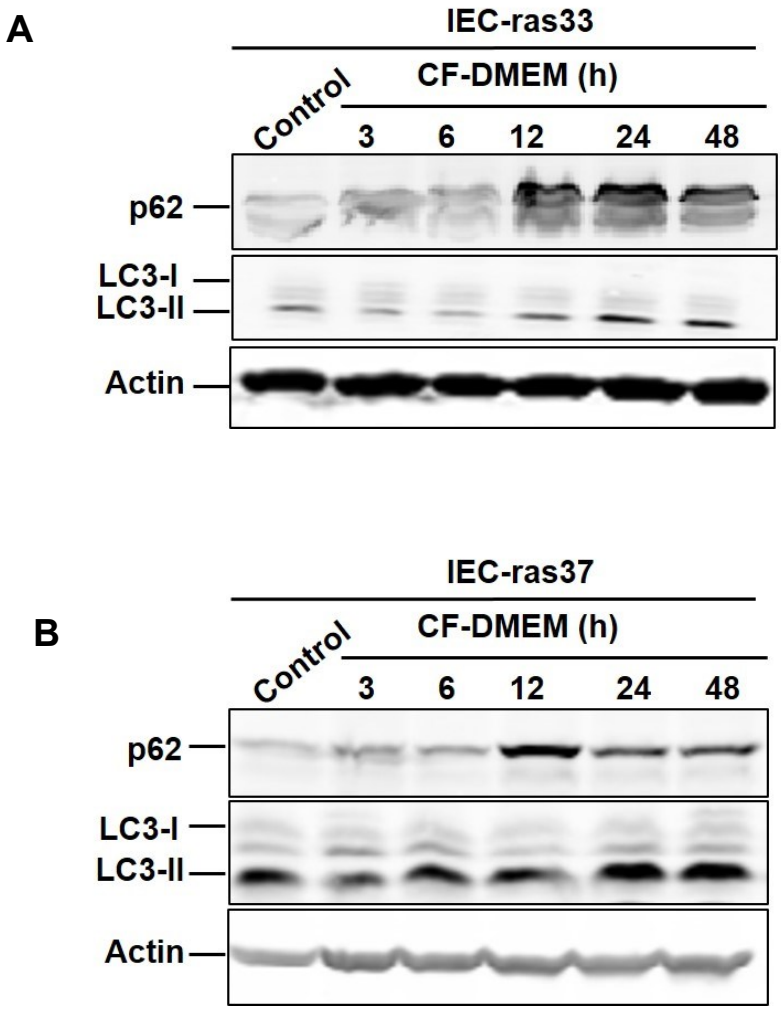

Figure 3.2.4: Effect of choline depletion on p62/SQSTM1 and LC3-II in IEC-ras33 and IEC-ras37. IEC-ras33 and IEC-ras37 were cultured in the absence of choline for the indicated times. Controls were cultured in choline for 48 h. Cells were then harvested, lysed in SDS-PAGE buffer, SDS-PAGE, immunoblotted for p62/SQSTM1, LC3 and actin. immunoblots were visualized by Odyssey infrared imaging system.

lysosome fusion, CQ would have no effect on p62/SQSTM1 levels. I observed that in medium with choline, p62/SQSTM1 and LC3-II were low and addition of CQ to cells, resulted in increased p62/SQSTM1 and LC3-II (**Figure 3.2.5**). These data show that CQ blocked autophagic flux under normal conditions. In choline-depleted cells, p62/SQSTM1 and LC3-II were increased compared with cells cultured in choline but addition of CQ had no effect on p62/SQSTM1 and LC3-II levels (**Figure 3.2.5**). This indicates that increased p62/SQSTM1 and LC3-II in IEC-ras choline-depleted cells was the result of inhibition prior to the fusion of autophagosome with the lysosome.

To investigate whether suppression of autophagy in IEC-ras34 was associated with decreased PC, experiments were undertaken to study whether supplementing cells with lyso-PC could restore autophagy. Lyso-PC is converted to PC by lysophosphatidylcholine acyltransferase (LPCAT1), which is overexpressed in some human cancers, such as prostate and hepatocarcinoma (184, 185). To test this hypothesis, IEC-ras34 cells were cultured in the presence or absence of choline and lyso-PC for 24 h (**figure 3.2.6**). Similar to previous observations, choline depletion caused accumulation of p62/SQSTM1 and LC3-II. Choline supplementation resulted in p62/SQSTM1 degradation and a reduction in LC3-II. Lyso-PC also decreased p62/SQSTM1 and LC3-II to the same level as in cells cultured in choline.

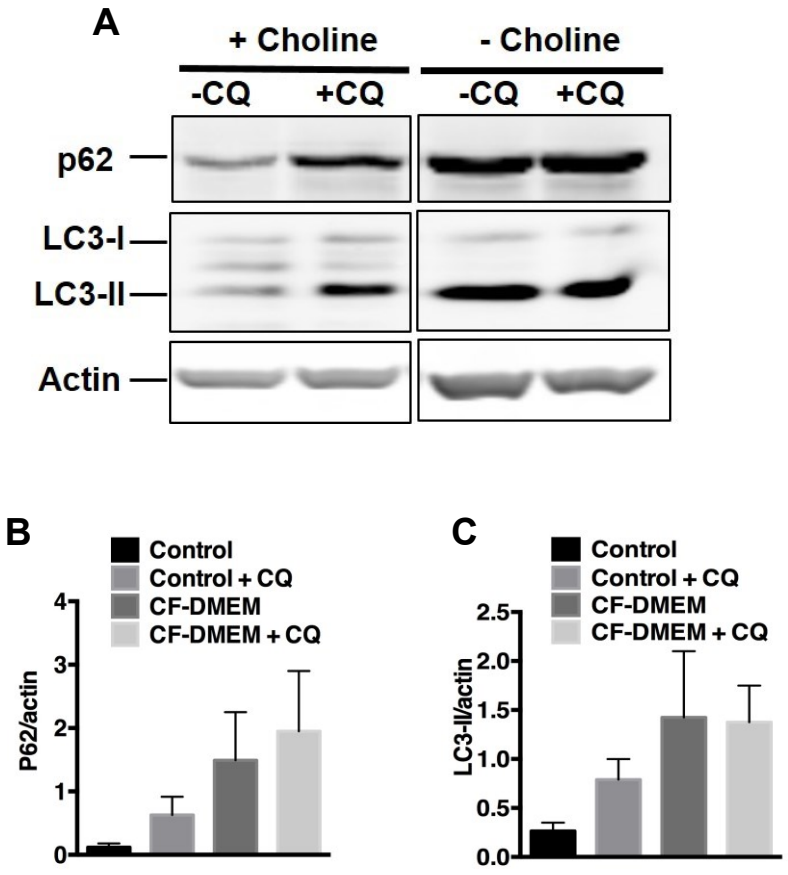

Figure 3.2.5: Inhibition of autophagic flux in IEC-ras34 cultured in the absence of choline. IEC-ras34 were grown in presence or absence of choline for 20 h. Cells were then treated with 400 μM of chloroquine (CQ) for 4 h, harvested, lysed in SDS-PAGE buffer, separated by SDS-PAGE, immunoblotted for p62/SQSTM1, LC3 and actin. Immunoblots were visualized by Odyssey infrared imaging system. Results are the mean and range of two independent experiments. Controls (cells cultured in 40 μM choline for 20 h)

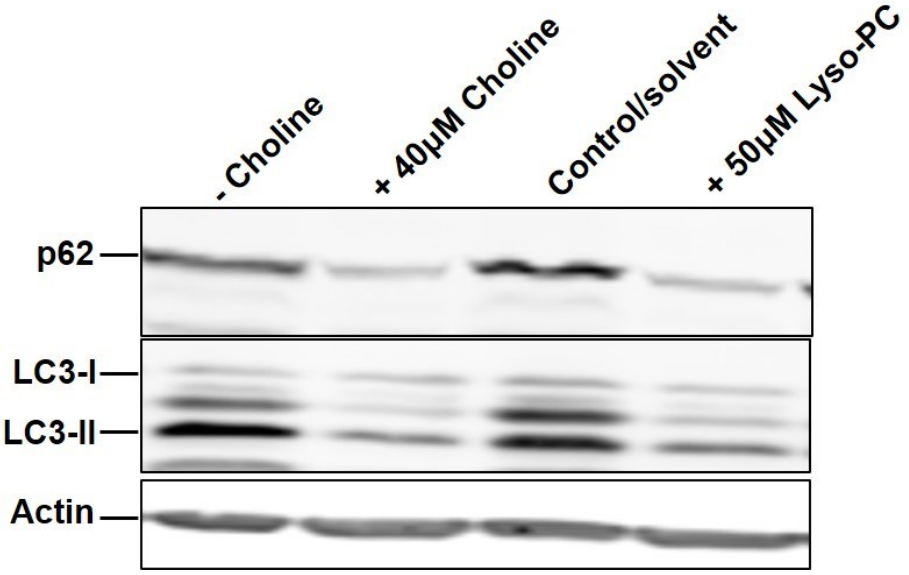

Figure 3.2.6: Effect of lyso-PC on autophagic markers in IEC-ras34. Cells were cultured in presence or absence of choline (40 μM) and lyso-PC (50 μM) for 24 h. Cells were then harvested, lysed in SDS-PAGE buffer, separated by SDS-PAGE, immunoblotted for p62/SQSTM1, LC3 and actin. Immunoblots were visualized by Odyssey infrared imaging system.

3.3 The effect of choline depletion on the proliferation of IEC-18 and IEC-ras34 cells

It is known that autophagy promotes cancer cells survival and proliferation, and its inhibition induces cell death (182). Since disruption of PC biosynthesis by choline depletion suppressed autophagy, it is possible that cell proliferation and survival of IEC-ras34 and IEC-18 were affected. To investigate whether choline depletion affects cell proliferation, IEC-18 and IEC-ras34 cell number was measured when cultured in DMEM with or without choline for up to 48 h. Choline-depleted IEC-18 were dividing similar to their choline supplemented control until 24 h, and then the number of cells remained constant at 48 h (**Figure 3.3.1.A**). The growth of choline-depleted and choline supplemented IEC-ras34 cells was similar until 12 h, after which control cells showed a 3-fold doubling but choline-depleted cells remained unchanged to 48 h (**Figure 3.3.1.B**). These data suggest that IEC-ras34 cells were more sensitive to choline depletion than IEC-18.

Finally, the effect of choline depletion on anchorage-dependent cell death (anoikis) in IEC-ras34 cells was tested. Since disruption of PC biosynthesis by knocking down CCTα sensitizes cells to anoikis. disruption of PC biosynthesis by choline depletion might lead to a similar effect. A clonogenicity assay was used to test whether choline depletion sensitizes IEC-ras34 to anoikis. This assay examines the anoikis resistance of cells and their ability to adhere and form colonies after detachment for up to 72 h. In this assay, IEC-ras34 cells were cultured in the presence or absence of choline while detached from the ECM (cultured on SP-agarose) for up to 72 h and then plated on plastic dishes to form colonies. While IEC-ras34 cultured in normal media survived over the 72 h time

course, cells cultured in the absence of choline displayed a 45 and 75% reduction in colony formation at 12 and 72 h, respectively, indicating increased sensitivity to anoikis (**figure 3.3.2**).

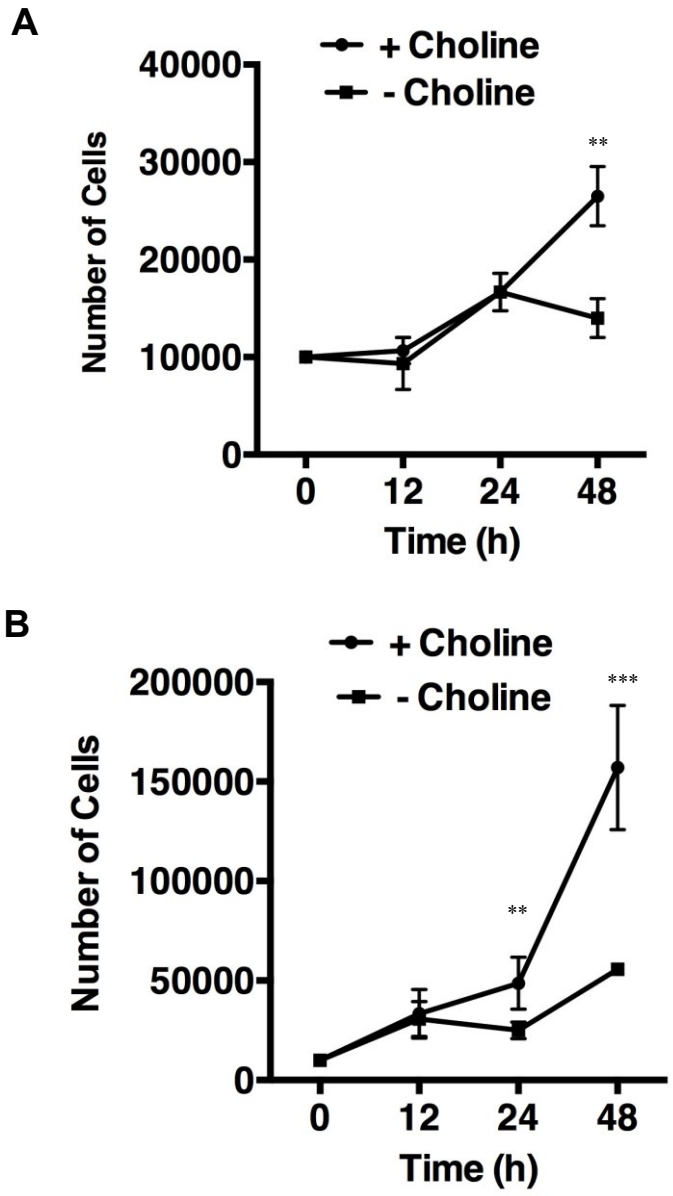

Figure 3.3.1: Choline depletion suppressed proliferation of IEC-ras34. IEC-18 (**A**) and IEC-ras34 (**B**) were cultured in the presence and absence of choline for the indicated times. Cells were then trypsinized, collected and counted using a haemocytometer. The number of choline-depleted cells was then compared to the control (cells cultured in choline) (see section 2.11). Results are the mean and SEM of three independent experiments. $^{**}p < 0.05$ and *** $p < 0.01$ compared with choline supplemented cells for each time point.

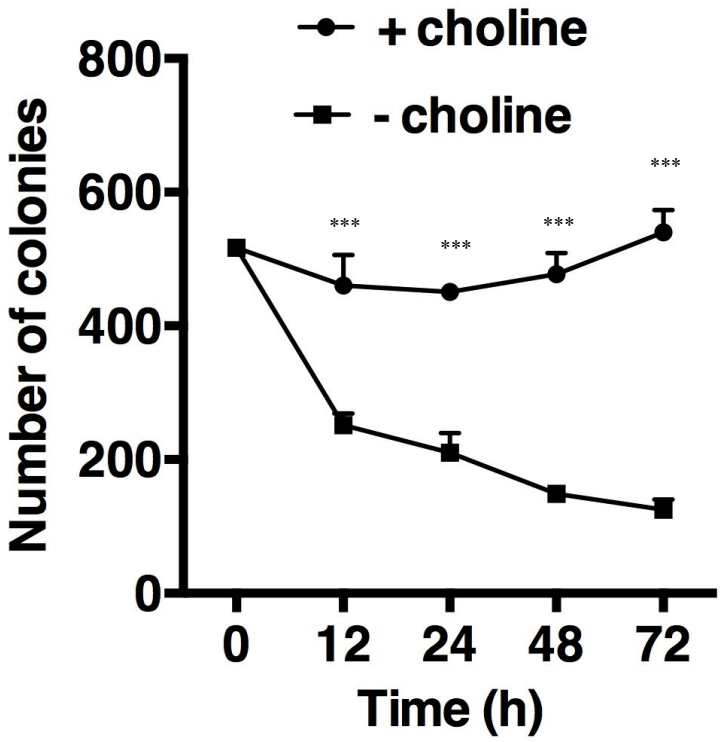

Figure 3.3.2: Choline depletion sensitizes IEC-ras34 cells to anoikis. IEC-ras34 were cultured in the presence or absence of choline on dishes coated with 1% SP-agarose for the indicated times, transferred to plastic dishes for 4 days. Colonies were quantified and compared to cells cultured in plastic dishes that were not detached. Results are the mean and SEM of three independent experiments. **, $p < 0.05$ and ***, $p < 0.01$ compared with control (cells were not detached).

CHAPTER 4 DISCUSSION

4.1 The role of CCTα in autophagy regulation in IEC-ras cells.

In eukaryotes, PC is the main constituent of membrane lipids, and is implicated in cell division and proliferation, either directly or through its catabolism (7). In mammalian cells, PC is produced by the CDP-choline pathway, where CCTα is the rate-limiting enzyme. Increased lipogenesis, including elevated fatty acid and PC biosynthesis, is a phenotype of cancer cells that was suggested to promote proliferation and apoptosis evasion (174). Transformation of epithelial cells with oncogenic ras increases PC synthesis by overexpression and/or activation of CKα and CCTα (39, 174). In addition, ras oncogene enhanced autophagy as a pro-survival mechanism, a process where the cell degrades its damaged organelles and long-lived proteins by packaging them in autophagosomes (186). The autophagosome double membrane likely originates in the ER (158), the primary site of PC synthesis, thus linking the CDP-choline pathway to early stages of autophagy. Therefore, it is possible that the up-regulation of CCTα and PC biosynthesis drive autophagy in IEC-ras by providing lipid for the autophagosomal double membrane.

In this study, transformation of IEC-18 with oncogenic H-ras increased ATG5 and ATG7 expression compared to normal IEC-18, indicating that autophagy was upregulated (**Figure 3.1.1)**. Adherent IEC-shNT had low autophagy flux based on low expression of p62/SQSTM1 and LC3-II. Upon detachment, IEC-shNT accumulated p62/SQST1 and LC3-II after 12 h, indicating impairment of autophagy (**Figure 3.1.3.A**). Previous work showed that IEC-18 had dramatically reduced PC biosynthesis and

increased anoikis after detachment compared with adherent cells (39). Therefore, impairment of autophagy in detached IEC-shNT could be linked to reduced PC synthesis. It was not surprising that CCTα knockdown in IEC-18 resulted in the same phenotype as control cells (**Figure 3.1.3.B**), since PC synthesis was already inhibited by detachment. It seems that CCTα knockdown had no effect on autophagic flux in adherent and detached IEC-18. Contrary to my findings, a study found that autophagy was induced in MCF10A breast epithelial cells after detachment (179). However, the limitation of that study was that LC3 was the only marker used, and increased LC3-II could mean either an increase or decrease in autophagic flux. Detachment of IEC-shNT and IEC-shCCTα from ECM resulted in PARP1 cleavage to the 89 kD fragment (**Figure 3.1.6.A)**, indicating that these cells were undergoing anoikis, possibly due to impaired autophagy induced by low PC biosynthesis. Overall, I observed a correlation between reduced PC synthesis in IEC-18 (shNT and shCCTα), impaired autophagy and induction of anoikis.

IEC-ras34 are anoikis resistant and grow in three-dimensional masses when deprived of contact with the ECM. The elevated ATG5 and ATG7 in IEC-ras34 suggest that autophagy was induced compared to IEC-18. When autophagy was tested in adherent IEC-ras-shNT, LC3-II was high and p62/SQSTM was degraded, confirming the induction of autophagy (**Figure 3.1.3.A** and **Figure 3.1.4**). This result was similar to a previous study that found H-ras upregulated basal autophagy that was required for cell survival (186). The degradation of p62/SQSTM1 in detached IEC-ras-shNT indicated that autophagy was also upregulated after detachment (**Figure 3.1.3**). This result is consistent with previous work showing that detachment upregulated autophagy in IEC-ras cells (176). In addition, PC biosynthesis was increased by 2-fold in detached IEC-ras34

compared with adherent cells (39). Therefore, it was not surprising that targeting CCTα by shRNA, which decreased PC biosynthesis, caused p62/SQSTM1 accumulation in adherent and detached cells (**Figure 3.1.3.A** and **Figure 3.1.4**), indicating that autophagy was impaired, presumably due to reduced PC levels. The cleavage of beclin1 in adherent and detached cells, which was correlated with p62/SQSTM1 accumulation, is another indication of deactivation of autophagy (**Figure 3.1.5**). A number of studies have previously shown that the cleavage of beclin1 by caspases resulted in autophagy down-regulation (187, 188). The beclin1 fragment does not induce autophagy but translocates to mitochondria, where it triggers cyt c release and induction of apoptosis. PARP1 cleavage was used to investigate whether CCTα knockdown induced anoikis in IEC-ras34. Cleavage of PARP1, commonly used as a marker of apoptosis, was increased in IEC-ras-shCCTα compared to shNT controls (**Figure 3.1.6.B**). The cleavage of PARP1 indicates increased susceptibility to anoikis, which might be due to impairment of autophagy triggered by reduced PC biosynthesis.

4.2. The effect of choline depletion on autophagy in IEC-18 and malignant IEC-ras34

To confirm that impairment of autophagy in CCTα knockdown IEC-ras34 was due to reduced PC biosynthesis, cells were depleted of choline while CCTα was active. Since ATG5 and ATG7 are elevated in IEC-ras34 compared with IEC-18, I expected that this elevation could be due to the increased PC caused by overexpression of CCTα. However, choline depletion did not affect ATG5 and ATG7 in IEC-ras34, meaning that reduced PC biosynthesis due to choline depletion was not involved in induction of these proteins

(**Figure 3.2.1**). However, depletion of choline caused p62/SQSTM1 and LC3-II accumulation in IEC-ras clones but not in control IEC-18 (**Figure 3.2.2**, **Figure 3.2.3** and **Figure 3.2.4**). It is rational to link the impairment of autophagy to the reduced PC biosynthesis since disruption of PC biosynthesis by CCTα knockdown in IEC-ras34 had a similar affect. In adherent IEC-18 the level of autophagic flux and CCTα are low, therefore, disruption of PC biosynthesis by either CCTα knockdown or choline depletion had no effect. In contrast, ras oncogene induces CCTα to increase PC needed to maintain high autophagic flux.

The increase of p62/SQSTM1 and LC3-II observed in CCTα knockdown or choline-depleted conditions indicate a suppression of autophagy. However, these proteins could also accumulate due to increased autophagic flux. To differentiate between these possibilities, CQ was used to block the fusion of autophagosomes with lysosomes. In cells cultured in choline, where the autophagic flux is normal, CQ is expected to stop p62/SQSTM1 degradation and LC3-II cycling. This was observed here, indicating that CQ blocked autophagy in cells cultured in the presence of choline. On the other hand, if increased p62/SQSTM1 and LC3-II in choline-depleted cells was due to decreased lysosomal function, addition of CQ should enhance the accumulation. However, treating IEC-ras34 with CQ in the absence of choline did not affect p62/SQSTM1 and LC3-II levels (**Figure 3.2.5**), indicating that suppression of autophagy occurs at or before the lysosome fusion step.

Choline depletion decreases PC but also reduces other metabolites of CDP-choline pathway such as phosphocholine and CDP-choline, as well as one-carbon metabolites

that are derived from choline (189). Therefore, the suppression of autophagy could be because of a reduction in one of these metabolites, or absence of choline itself. To show that PC was the required product that prevented the block in autophagy, IEC-ras34 were supplemented with lyso-PC, which is converted to PC by LPCAT1. This approach restored autophagy as indicated by the return of p62/SQSTM1 and LC3-II level to those found in cells cultured in choline (**Figure 3.2.6**). This provides evidence that the reduction of PC biosynthesis in choline-depleted cells caused the suppression of autophagy at or prior to fusion of the autophagosome with the lysosome.

These results raised a question, where exactly PC biosynthesis is involved in autophagy regulation? The suppression of autophagy might occur at an early stage, before phagophore initiation due to mTOR signaling. However, this possibility is weak because choline depletion did not affect ATG5 and ATG7 expression in IEC-ras34. In addition, I would expect to see an increase in LC3-I over LC3-II when the suppression takes place before LC3-I lipidation during the elongation step. However, in adherent IEC-ras-shCCTα cells, LC3-I was expressed, which could be because targeting CCTα does not stop the synthesis of PC completely. In addition, CCTβ is still active. Therefore, the amount of PC left in adherent IEC-ras-shCCTα is sufficient to allow LC3-II recycling. In the choline depletion model where PC synthesis is completely blocked, LC3-I was not detectable, meaning that recycling of LC3-II to LC3-I was inhibited. The second possibility is that PC is involved in synthesis of autophagosomal double membranes, and that reduced PC level suppressed synthesis of autophagosomal double membranes at the elongation step. In support of this concept, the lipidation of LC3-I takes place at the elongation step and that is why there was an increase in LC3-II and p62/SQSTM1 in

IEC-ras34 cultured without choline. As well, PC biosynthesis by CEPT occurs in the ER, the site of phagophore initiation. The synthesis of PE and PI3K, two phospholipids involved in autophagy regulation, also occurs in the ER. The third possibility is that autophagosome could be formed completely but reduced PC impairs lysosomal function, resulting in inhibition of fusion with the autophagosome and degradation of p62/SQSTM1 and LC3-II recycling. I used electron microscopy (EM) to see if autophagosomes were present in IEC-ras34 cultured in the absence of choline but it was difficult to interpret the results (not shown). Expression of GFP-LC3 or mCherry-GFP-LC3 could be useful to determine if autophagosomes are formed under conditions of reduced PC synthesis.

4.3 The effect of choline depletion on the growth of control and IEC-ras transformed cells

Late in the G2/M phase of the cell cycle, PC synthesis is increased to double membrane mass that is required for cell division (11). When cultured in the same medium, the proliferation of IEC-ras34 cells is three times higher than IEC-18. Therefore, IEC-ras34 have increased CCTα expression and PC biosynthesis to compensate for the high rate of proliferation. A finding of this study was that IEC-ras34 cells were more sensitive to choline depletion. Choline depletion had no effect on the proliferation of IEC-18 cells until 24 h. In contrast, choline-depleted IEC-ras34 exhibited growth suppression by 50% compared to cells cultured in choline at 24 h (**Figure 3.3.1**). In addition to a cell cycle requirement for PC, we showed that PC is also required for autophagy, potentially linking these two processes.

Finally, choline depletion was found to sensitize IEC-ras34 cells to anoikis (**Figure 3.3.2**). This result was consistent with previous study that showed CCTα silencing induced anoikis in IEC-ras34 (39). Detachment of ras-transformed cells from ECM is known to induce autophagy, which then helps the cells to resist anoikis (176). In that study, targeting autophagy genes induced anoikis. Similarly, disruption of PC biosynthesis by choline depletion suppressed autophagy and then induced anoikis in IEC-ras34 cells. **Figure 4** shows a model that describes the relationship between autophagy-related anoikis resistance and the PC biosynthesis in ras-transformed cancer cells.

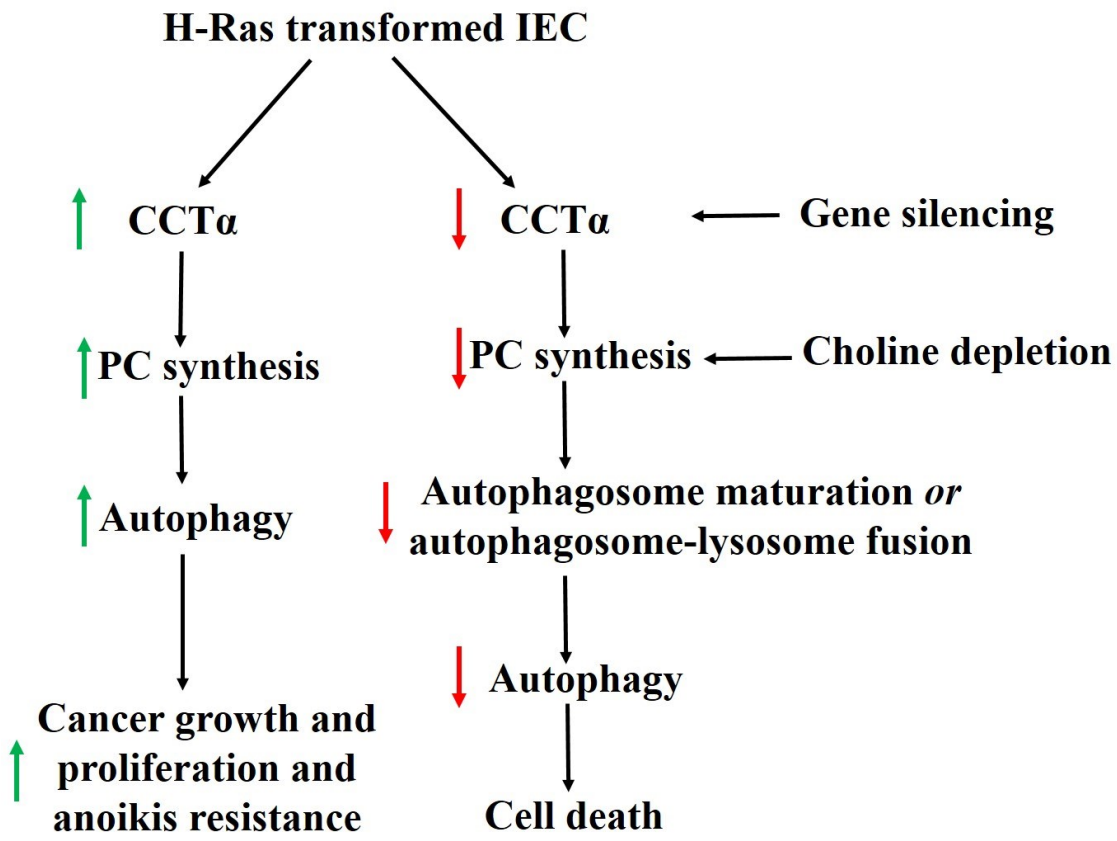

Figure 4: The involvement of PC biosynthesis in regulation of H-ras induced autophagy and anoikis in IEC-ras34. Oncogenic H-ras increased PC biosynthesis in IEC by promoting the expression of CCTα, which then upregulates autophagy and promotes anoikis resistance. In contrast, targeting PC biosynthesis by CCTα knockdown or choline depletion downregulated autophagy and induced cell death.

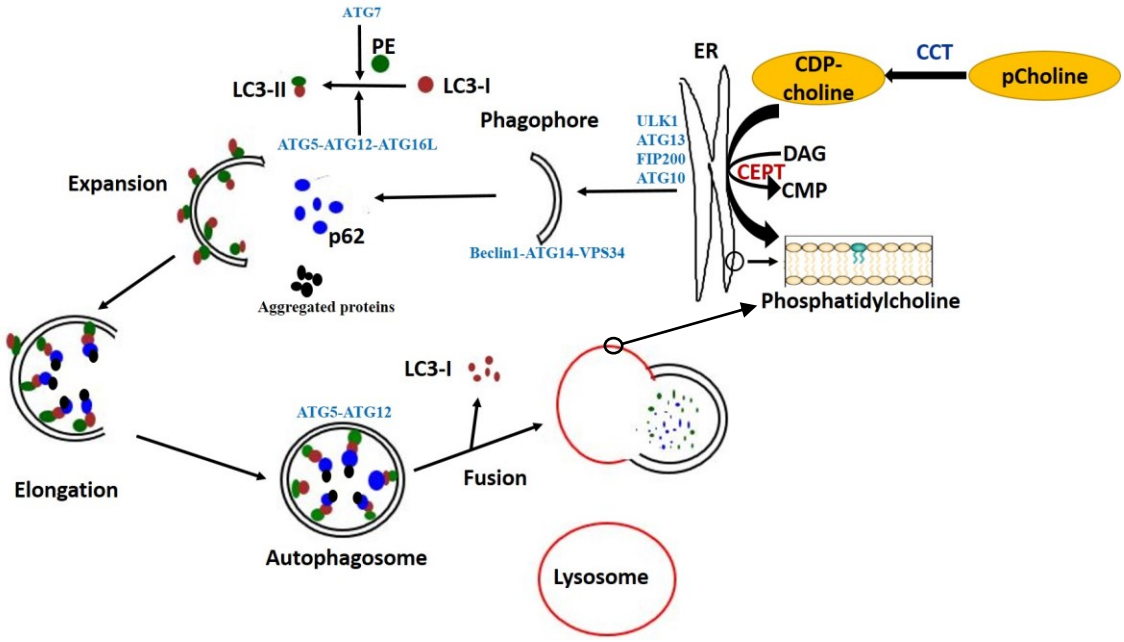

Figure 5: The relationship between the PC biosynthesis and autophagy. The final step of PC biosynthesis and phagophore formation take place at the ER. PC biosynthesis could be involved in formation of the autophagosomal membranes, or might be necessary for lysosomal membrane biogenesis.

CHAPTER 5 CONCLUSION

In this study, I showed that reducing CCTα expression in IEC-ras34 suppressed autophagy and enhanced anoikis, indicating a link to reduced PC biosynthesis. Similarly, disruption of PC biosynthesis by choline depletion inhibited autophagy prior to fusion of autophagosomes with lysosomes in IEC-ras34 but not IEC-18. IEC-ras34 were more sensitive to choline depletion compared to IEC-18 because IEC-ras34 require more PC to compensate the high cell proliferation rate and autophagy. Similarly, depletion of choline induced anoikis in IEC-ras34, which could be due to suppression of autophagy. Overall, these data indicate that PC plays a pivotal role in regulation of autophagy in IEC-ras. Targeting PC biosynthesis may offer a novel approach to limit the growth of cancer cells while sparing non-proliferative, normal cells.

REFERENCES

1. Van Meer G, Voelker DR, Feigenson GW. **Membrane lipids: where they are and how they behave**. Nature. Rev. *Mol. Cell Biol*. 2008;9:112-24.

2. Fadok VA, Voelker DR, Campbell PA, Cohen JJ, Bratton DL, Henson PM. **Exposure of phosphatidylserine on the surface of apoptotic lymphocytes triggers specific recognition and removal by macrophages**. *J Immunol*. 1992;148:2207-16.

3. Daleke DL. **Regulation of transbilayer plasma membrane phospholipid asymmetry**. *J Lipid Res*. 2003;44:233-42.

4. Cote GG, Crain RC. **Biochemistry of phosphoinositides**. *Annual Rev plant Biol*. 1993;44:333-56.

5. Cornell RB, Ridgway ND. **CTP:phosphocholine cytidylyltransferase: Function, regulation, and structure of an amphitropic enzyme required for membrane biogenesis**. *Prog Lipid Res.* 2015;59:147-71.

6. Kagan VE, Tyurin VA, Jiang J, Tyurina YY, Ritov VB, Amoscato AA, et al. **Cytochrome c acts as a cardiolipin oxygenase required for release of proapoptotic factors**. *Nature Chem. Bio*. 2005;1:223-32.

7. Lin W, Arthur G. **Phospholipids are synthesized in the G2/M phase of the cell cycle**. *Int J Biochem Cell Biol*. 2007;39:597-605.

8. Cullis Pt, Kruijff Bd. **Lipid polymorphism and the functional roles of lipids in biological membranes**. *Biochim. Biophys. Acta*. 1979;559:399-420.

9. Nakamura T, Lin LL, Kharbanda S, Knopf J, Kufe D. **Macrophage colony stimulating factor activates phosphatidylcholine hydrolysis by cytoplasmic phospholipase A2**. *EMBO J*. 1992 ;11:4917-22.

10. Monick MM, Carter AB, Gudmundsson G, Mallampalli R, Powers LS, Hunninghake GW. **A phosphatidylcholine-specific phospholipase C regulates activation of p42/44 mitogen-activated protein kinases in lipopolysaccharide-stimulated human alveolar macrophages**. J Immunol. 1999;162:3005-12.

11. Liscovitch M, Ben-Av P, Danin M, Faiman G, Eldar H, Livneh E. **Phospholipase D-mediated hydrolysis of phosphatidylcholine: role in cell signalling**. J Lipid Mediat. 1993 Nov;8:177-82.

12. Wu D, Hersh LB. **Choline acetyltransferase: celebrating its fiftieth year**. *J Neurochem*. 1994;62:1653-63.

13. Zeisel SH. **Choline: needed for normal development of memory**. *J Am Coll Nutr*. 2000;19:528S-31S.

14. Zeisel SH. **Choline: critical role during fetal development and dietary requirements in adults**. *Annu Rev Nutr*. 2006;26:229-50.

15. Fischer LM, Scearce JA, Mar MH, Patel JR, Blanchard RT, Macintosh BA, et al. **Ad libitum choline intake in healthy individuals meets or exceeds the proposed adequate intake level**. *J Nutr*. 2005;135:826-9.

16. Li Z, Vance DE. **Phosphatidylcholine and choline homeostasis**. *J Lipid Res*. 2008;49:1187-94.

18. Vance DE, Ridgway ND. **The methylation of phosphatidylethanolamine**. *Prog Lipid Res.* 1988;27:61-79.

19. Horl G, Wagner A, Cole LK, Malli R, Reicher H, Kotzbeck P, et al. **Sequential synthesis and methylation of phosphatidylethanolamine promote lipid droplet biosynthesis and stability in tissue culture and in vivo**. *J Biol Chem*. 2011;286:17338-50.

20. Cui Z, Vance JE, Chen MH, Voelker DR, Vance DE. **Cloning and expression of a novel phosphatidylethanolamine N-methyltransferase. A specific biochemical and cytological marker for a unique membrane fraction in rat liver**. *J Biol Chem*. 1993 268:16655-63.

21. Zhu X, Song J, Mar MH, Edwards LJ, Zeisel SH. **Phosphatidylethanolamine N-methyltransferase (PEMT) knockout mice have hepatic steatosis and abnormal hepatic choline metabolite concentrations despite ingesting a recommended dietary intake of choline**. *Biochem J*. 2003;370:987-93.

22. Noga AA, Zhao Y, Vance DE. **An unexpected requirement for phosphatidylethanolamine N-methyltransferase in the secretion of very low density lipoproteins**. *J Biol Chem*. 2002;277:42358-65.

23. Jacobs RL, Zhao Y, Koonen DP, Sletten T, Su B, Lingrell S, et al. **Impaired de novo choline synthesis explains why phosphatidylethanolamine N-methyltransferase-deficient mice are protected from diet-induced obesity**. *J Biol Chem*. 2010;285:22403-13.

24. DeLong CJ, Shen YJ, Thomas MJ, Cui Z. **Molecular distinction of phosphatidylcholine synthesis between the CDP-choline pathway and phosphatidylethanolamine methylation pathway**. *J Biol Chem*. 1999;274:29683-8.

25. Simon J, Atweh S, Kuhar M. **Sodium-dependent high affinity choline uptake: a regulatory step in the synthesis of acetylcholine**. *J Neurochem*. 1976;26:909-22.

26. Michel V, Yuan Z, Ramsubir S, Bakovic M. **Choline transport for phospholipid synthesis**. *Exp Biol Med* . 2006;231:490-504.

27. Ridgway N, McLeod R. **Biochemistry of lipids, lipoproteins and membranes**. Elsevier; 2015.

28. Aoyama C, Liao H, Ishidate K. **Structure and function of choline kinase isoforms in mammalian cells**. *Prog Lipid Res*. 2004;43:266-81.

29. Wu G, Aoyama C, Young SG, Vance DE. **Early embryonic lethality caused by disruption of the gene for choline kinase alpha, the first enzyme in phosphatidylcholine biosynthesis**. *J Biol Chem*. 2008;283:1456-62.

30. Ratnam S, Kent C. **Early Increase in Choline Kinase Activity upon Induction of the H-rasOncogene in Mouse Fibroblast Cell Lines**. *Arch Biochem Biophys*. 1995;323:313-22.

31. Shah T, Wildes F, Penet M, Winnard PT, Glunde K, Artemov D, et al. **Choline kinase overexpression increases invasiveness and drug resistance of human breast cancer cells**. *NMR Biomed*. 2010;23:633-42.

32. Mitsuhashi S, Ohkuma A, Talim B, Karahashi M, Koumura T, Aoyama C, et al. **A congenital muscular dystrophy with mitochondrial structural abnormalities caused by defective de novo phosphatidylcholine biosynthesis**. *The Ameri J Hum Genes*. 2011;88:845-51.

33. Lykidis A, Murti KG, Jackowski S. **Cloning and characterization of a second human CTP: phosphocholine cytidylyltransferase**. *J Biol Chem*. 1998;273:14022-9.

34. Tang W, Keesler GA, Tabas I. **The Structure of the Gene for Murine CTP: Phosphocholine Cytidylyltransferase, Ctpct**. *J Biol Chem*. 1997;272:13146-51.

35. Lykidis A, Jackson P, Jackowski S. **Lipid activation of CTP: phosphocholine cytidylyltransferase α: characterization and identification of a second activation domain**. *Biochemistry*. 2001;40:494-503.

36. Jackowski S, Rehg JE, Zhang YM, Wang J, Miller K, Jackson P, et al. **Disruption of CCTbeta2 expression leads to gonadal dysfunction**. *Mol Cell Biol*. 2004;24:4720-33.

37. Agassandian M, Mallampalli RK. **Surfactant phospholipid metabolism**. *Biochim Biophys Acta*. 2013;1831:612-25.

38. Tian Y, Zhou R, Rehg JE, Jackowski S. **Role of phosphocholine cytidylyltransferase alpha in lung development**. *Mol Cell Biol*. 2007;27:975-82.

39. Arsenault DJ, Yoo BH, Rosen KV, Ridgway ND. **ras-Induced up-regulation of CTP:phosphocholine cytidylyltransferase alpha contributes to malignant transformation of intestinal epithelial cells**. *J Biol Chem*. 2013;288:633-43.

40. Cui Z, Houweling M, Chen MH, Record M, Chap H, Vance DE, et al. **A genetic defect in phosphatidylcholine biosynthesis triggers apoptosis in Chinese hamster ovary cells**. *J Biol Chem*. 1996 ;271:14668-71.

41. Wang Y, MacDonald JI, Kent C. **Identification of the nuclear localization signal of rat liver CTP: phosphocholine cytidylyltransferase**. *J Biol Chem*. 1995;270:354-60.

42. Fagone P, Gunter C, Sage CR, Gunn KE, Brewer JW, Jackowski S. **CTP:phosphocholine cytidylyltransferase alpha is required for B-cell proliferation and class switch recombination**. *J Biol Chem*. 2009;284:6847-54.

43. Lagace TA, Miller JR, Ridgway ND. **Caspase processing and nuclear export of CTP:phosphocholine cytidylyltransferase alpha during farnesol-induced apoptosis**. *Mol Cell Biol*. 2002;22:4851-62.

44. Kalmar GB, Kay RJ, LaChance AC, Cornell RB. **Primary structure and expression of a human CTP: phosphocholine cytidylyltransferase**. *Biochim. Biophys. Acta*. 1994;1219:328-34.

45. Xie M, Smith JL, Ding Z, Zhang D, Cornell RB. **Membrane binding modulates the quaternary structure of CTP:phosphocholine cytidylyltransferase**. *J Biol Chem*. 2004;279:28817-25.

46. Helmink BA, Braker JD, Kent C, Friesen JA. **Identification of lysine 122 and arginine 196 as important functional residues of rat CTP: phosphocholine cytidylyltransferase alpha**. *Biochemistry*.;42:5043-51.

47. Clement JM, Kent C. **CTP: phosphocholine cytidylyltransferase: insights into regulatory mechanisms and novel functions**. *Biochem. Biophys. Res. Commun*. 1999;257:643-50.

48. Johnson JE, Cornell RB. **Membrane-binding amphipathic. alpha.-helical peptide derived from CTP: Phosphocholine cytidylyltransferase**. *Biochemistry*. 1994;33:4327-35.

49. Cornell RB, Northwood IC. **Regulation of CTP: phosphocholine cytidylyltransferase by amphitropism and relocalization**. *Trends Biochem Sci*. 2000;25:441-7.

50. Wang Y, Kent C. **Identification of an inhibitory domain of CTP:phosphocholine cytidylyltransferase**. *J Biol Chem*. 1995;270:18948-52.

51. Wang Y, Kent C. **Effects of altered phosphorylation sites on the properties of CTP:phosphocholine cytidylyltransferase**. *J Biol Chem*. 1995;270:17843-9.

52. Jackowski S. **Coordination of membrane phospholipid synthesis with the cell cycle**. *J Biol Chem*. 1994;269:3858-67.

53. Yang W, Jackowski S. **Lipid activation of CTP: phosphocholine cytidylyltransferase is regulated by the phosphorylated carboxyl-terminal domain**. *J Biol Chem*. 1995;270:16503-6.

54. McMaster CR, Bell RM. **CDP-choline: 1, 2-diacylglycerol cholinephosphotransferase**. *Biochim. Biophys. Acta*. 1997;1348:100-10.

55. Henneberry A, McMaster C. **Cloning and expression of a human choline/ethanolaminephosphotransferase: synthesis of phosphatidylcholine and phosphatidylethanolamine**. 1999;339:291-8.

56. Jamil H, Utal AK, Vance DE. **Evidence that cyclic AMP-induced inhibition of phosphatidylcholine biosynthesis is caused by a decrease in cellular diacylglycerol levels in cultured rat hepatocytes**. *J Biol Chem*. 1992;267:1752-60.

57. Houweling M, Cui Z, Vance DE. **Expression of phosphatidylethanolamine N-methyltransferase-2 cannot compensate for an impaired CDP-choline pathway in mutant Chinese hamster ovary cells**. *J Biol Chem*. 1995;270:16277-82.

58. Yamamoto T, Taya S, Kaibuchi K. **Ras-induced transformation and signaling pathway**. *J Biochem*. 1999;126:799-803.

59. Macara IG. **Elevated phosphocholine concentration in ras-transformed NIH 3T3 cells arises from increased choline kinase activity, not from phosphatidylcholine breakdown**. *Mol Cell Biol*. 1989;9:325-8.

60. Sugimoto H, Banchio C, Vance DE. **Transcriptional regulation of phosphatidylcholine biosynthesis**. *Prog Lipid Res*. 2008;47:204-20.

61. Bakovic M, Waite K, Vance DE. **Oncogenic Ha-Ras transformation modulates the transcription of the CTP:phosphocholine cytidylyltransferase alpha gene via p42/44MAPK and transcription factor Sp3**. *J Biol Chem*. 2003;278:14753-61.

62. Kaplan DR, Whitman M, Schaffhausen B, Pallas DC, White M, Cantley L, et al. **Common elements in growth factor stimulation and oncogenic transformation: 85 kd phosphoprotein and phosphatidylinositol kinase activity**. *Cell*. 1987;50:1021-9.

63. Martini M, De Santis MC, Braccini L, Gulluni F, Hirsch E. **PI3K/AKT signaling pathway and cancer: an updated review**. *Ann Med*. 2014;46:372-83.

64. Cairns RA, Harris IS, Mak TW. **Regulation of cancer cell metabolism**. *Nat Rev Canc*. 2011;11:85-95.

65. Wang T, Li J, Chen F, Zhao Y, He X, Wan D, et al. **Choline transporters in human lung adenocarcinoma: expression and functional implications**. *Biochim et Biophys Acta*. 2007;39:668-74.

66. Yalcin A, Clem B, Makoni S, Clem A, Nelson K, Thornburg J, et al. **Selective inhibition of choline kinase simultaneously attenuates MAPK and PI3K/AKT signaling**. *Oncogene*. 2010;29:139-49.

67. Elmore S. **Apoptosis: a review of programmed cell death**. *Toxicol Pathol*. 2007;35: 495-516.

68. Shanmugathasan M, Jothy S. **Apoptosis, anoikis and their relevance to the pathobiology of colon cancer**. *Pathol Int*. 2000;50:273-9.

69. Shiozaki EN, Chai J, Shi Y. **Oligomerization and activation of caspase-9, induced by Apaf-1 CARD**. *Proc Natl Acad Sci*. 2002;99:4197-202.

70. Bodmer J, Holler N, Reynard S, Vinciguerra P, Schneider P, Juo P, et al. **TRAIL receptor-2 signals apoptosis through FADD and caspase-8**. *Nat Cell Biol*. 2000;2:241-3.

71. Yen CL, Mar MH, Zeisel SH. **Choline deficiency-induced apoptosis in PC12 cells is associated with diminished membrane phosphatidylcholine and sphingomyelin, accumulation of ceramide and diacylglycerol, and activation of a caspase**. *FASEB J*. 1999;13:135-42.

72. Miquel K, Pradines A, Tercé F, Selmi S, Favre G. **Competitive inhibition of choline phosphotransferase by geranylgeraniol and farnesol inhibits phosphatidylcholine synthesis and induces apoptosis in human lung adenocarcinoma A549 cells**. *J Biol Chem*. 1998;273:26179-86.

73. Cui Z, Houweling M, Chen MH, Record M, Chap H, Vance DE, et al. **A genetic defect in phosphatidylcholine biosynthesis triggers apoptosis in Chinese hamster ovary cells**. *J Biol Chem*. 1996;271:14668-71.

74. Frisch SM, Francis H. **Disruption of epithelial cell-matrix interactions induces apoptosis**. *J Cell Biol*. 1994;124:619-26.

75. Strater J, Wedding U, Barth T, Koretz K, Elsing C, Moller P. **Rapid onset of apoptosis in vitro follows disruption of beta 1-integrin/matrix interactions in human colonic crypt cells**. *Gastroenterology*. 1996;110:1776-84.

76. Rosen K, Shi W, Calabretta B, Filmus J. **Cell detachment triggers p38 mitogen-activated protein kinase-dependent overexpression of Fas ligand. A novel mechanism of Anoikis of intestinal epithelial cells**. *J Biol Chem*. 2002;277:46123-30.

77. Valentijn AJ, Metcalfe AD, Kott J, Streuli CH, Gilmore AP. **Spatial and temporal changes in Bax subcellular localization during anoikis**. *J Cell Biol*. 2003;162:599-612.

78. Frisch SM, Vuori K, Kelaita D, Sicks S. **A role for Jun-N-terminal kinase in anoikis; suppression by bcl-2 and crmA**. *J Cell Biol*. 1996;135:1377-82.

79. Reginato MJ, Mills KR, Paulus JK, Lynch DK, Sgroi DC, Debnath J, et al. **Integrins and EGFR coordinately regulate the pro-apoptotic protein Bim to prevent anoikis**. *Nat Cell Biol*. 2003;5:733-40.

80. Rosen K, Rak J, Leung T, Dean NM, Kerbel RS, Filmus J. **Activated Ras prevents downregulation of Bcl-X(L) triggered by detachment from the extracellular matrix. A mechanism of Ras-induced resistance to anoikis in intestinal epithelial cells**. *J Cell Biol*. 2000;149:447-56.

81. Yoo BH, Wu X, Li Y, Haniff M, Sasazuki T, Shirasawa S, et al. **Oncogenic ras-induced down-regulation of autophagy mediator Beclin-1 is required for malignant transformation of intestinal epithelial cells**. *J Biol Chem*. 2010;285:5438-49.

83. He C, Klionsky DJ. **Regulation mechanisms and signaling pathways of autophagy**. *Annu Rev Genet*. 2009;43:67-93.

84. Ravikumar B, Sarkar S, Davies JE, Futter M, Garcia-Arencibia M, Green-Thompson ZW, et al. **Regulation of mammalian autophagy in physiology and pathophysiology**. *Physiol Rev*. 2010;90:1383-435.

85. Klionsky, D. J., Abdelmohsen, K., Abe, A., Abedin, M. J., Abeliovich, H., Acevedo Arozena, A., ... & Adhihetty, P. J. **Guidelines for the use and interpretation of assays for monitoring autophagy**. *Autophagy*. 2016; 12:1-222

86. Ylä-Anttila P, Vihinen H, Jokitalo E, Eskelinen E. **3D tomography reveals connections between the phagophore and endoplasmic reticulum**. *Autophagy*. 2009;5:1180-5.

87. Hayashi-Nishino M, Fujita N, Noda T, Yamaguchi A, Yoshimori T, Yamamoto A. **A subdomain of the endoplasmic reticulum forms a cradle for autophagosome formation**. *Nat Cell Biol*. 2009;11:1433-7.

88. Chang YY, Neufeld TP. **An Atg1/Atg13 complex with multiple roles in TOR-mediated autophagy regulation**. *Mol Biol Cell.* 2009;20:2004-14.

89. Kamada Y, Funakoshi T, Shintani T, Nagano K, Ohsumi M, Ohsumi Y. **Tor-mediated induction of autophagy via an Apg1 protein kinase complex**. *J Cell Biol*. 2000;150:1507-13.

90. Jung CH, Jun CB, Ro SH, Kim YM, Otto NM, Cao J, et al. **ULK-Atg13-FIP200 complexes mediate mTOR signaling to the autophagy machinery**. *Mol Biol Cell*. 2009;20:1992-2003.

91. Mercer CA, Kaliappan A, Dennis PB. **A novel, human Atg13 binding protein, Atg101, interacts with ULK1 and is essential for macroautophagy**. *Autophagy.* 2009;5:649-62.

92. Itakura E, Kishi C, Inoue K, Mizushima N. **Beclin 1 forms two distinct phosphatidylinositol 3-kinase complexes with mammalian Atg14 and UVRAG**. *Mol Biol Cell*. 2008;19:5360-72.

93. Sun Q, Fan W, Chen K, Ding X, Chen S, Zhong Q. **Identification of Barkor as a mammalian autophagy-specific factor for Beclin 1 and class III phosphatidylinositol 3-kinase**. *Proc Natl Acad Sci.* 2008;105:19211-6.

94. Furuya N, Yu J, Byfield M, Pattingre S, Levine B. **The evolutionarily conserved domain of Beclin 1 is required for Vps34 binding, autophagy, and tumor suppressor function**. *Autophagy*. 2005;1:46-52.

95. Pattingre S, Tassa A, Qu X, Garuti R, Liang XH, Mizushima N, et al. **Bcl-2 antiapoptotic proteins inhibit Beclin 1-dependent autophagy**. *Cell*. 2005;122:927-39.

96. Chang NC, Nguyen M, Germain M, Shore GC. **Antagonism of Beclin 1-dependent autophagy by BCL-2 at the endoplasmic reticulum requires NAF-1**. *EMBO J.* 2010;29:606-18.

97. Wei Y, Pattingre S, Sinha S, Bassik M, Levine B. J**NK1-mediated phosphorylation of Bcl-2 regulates starvation-induced autophagy**. *Mol Cell.* 2008;30:678-88.

98. Ravikumar B, Sarkar S, Davies JE, Futter M, Garcia-Arencibia M, Green-Thompson ZW, et al. **Regulation of mammalian autophagy in physiology and pathophysiology**. *Physiol Rev.* 2010;90:1383-435.

99. Mizushima N, Sugita H, Yoshimori T, Ohsumi Y. **A new protein conjugation system in human. The counterpart of the yeast Apg12p conjugation system essential for autophagy**. *J Biol Chem*. 1998;273:33889-92.

100. Mizushima N, Kuma A, Kobayashi Y, Yamamoto A, Matsubae M, Takao T, et al. **Mouse Apg16L, a novel WD-repeat protein, targets to the autophagic isolation membrane with the Apg12-Apg5 conjugate**. *J Cell Sci*. 2003;116:1679-88.

101. Saitoh T, Fujita N, Jang MH, Uematsu S, Yang B, Satoh T, et al. **Loss of the autophagy protein Atg16L1 enhances endotoxin-induced IL-1&bgr; production**. *Nature.* 2008;456:264-8.

102. Cadwell K, Liu JY, Brown SL, Miyoshi H, Loh J, Lennerz JK, et al. **A key role for autophagy and the autophagy gene Atg16l1 in mouse and human intestinal Paneth cells**. *Nature*. 2008;456:259-63.

103. Hemelaar J, Lelyveld VS, Kessler BM, Ploegh HL. **A single protease, Apg4B, is specific for the autophagy-related ubiquitin-like proteins GATE-16, MAP1-LC3, GABARAP, and Apg8L**. *J Biol Chem*. 2003;278:51841-50.

104. Kabeya Y, Mizushima N, Ueno T, Yamamoto A, Kirisako T, Noda T, et al. **LC3, a mammalian homologue of yeast Apg8p, is localized in autophagosome membranes after processing**. *EMBO J*. 2000;19:5720-8.

105. Tanida I, Sou YS, Ezaki J, Minematsu-Ikeguchi N, Ueno T, Kominami E. **HsAtg4B/HsApg4B/autophagin-1 cleaves the carboxyl termini of three human Atg8 homologues and delipidates microtubule-associated protein light chain 3- and GABAA receptor-associated protein-phospholipid conjugates**. *J Biol Chem*. 2004;279:36268-76.

106. Komatsu M, Ichimura Y. **Physiological significance of selective degradation of p62 by autophagy**. *FEBS Lett*. 2010;584:1374-8.

107. Itakura E, Mizushima N. **p62 Targeting to the autophagosome formation site requires self-oligomerization but not LC3 binding**. *J Cell Biol*. 2011;192:17-27.

108. Sanz L, Diaz-Meco MT, Nakano H, Moscat J. **The atypical PKC-interacting protein p62 channels NF-kappaB activation by the IL-1-TRAF6 pathway**. *EMBO J*. 2000;19:1576-86.

109. Rachubinski RA, Marcus SL, Capone JP. **The p56(lck)-interacting protein p62 stimulates transcription via the SV40 enhancer**. *J Biol Chem*. 1999;274:18278-84.

110. Pankiv S, Clausen TH, Lamark T, Brech A, Bruun JA, Outzen H, et al. **p62/SQSTM1 binds directly to Atg8/LC3 to facilitate degradation of ubiquitinated protein aggregates by autophagy**. *J Biol Chem*. 2007;282:24131-45.

111. Seibenhener ML, Babu JR, Geetha T, Wong HC, Krishna NR, Wooten MW. **Sequestosome 1/p62 is a polyubiquitin chain binding protein involved in ubiquitin proteasome degradation**. *Mol Cell Biol*. 2004;24:8055-68.

112. Manley S, Williams JA, Ding WX. **Role of p62/SQSTM1 in liver physiology and pathogenesis**. *Exp Biol Med*. 2013;238:525-38.

113. Goode A, Layfield R. **Recent advances in understanding the molecular basis of Paget disease of bone**. *J Clin Pathol*. 2010;63:199-203.

114. Durán A, Serrano M, Leitges M, Flores JM, Picard S, Brown JP, et al. **The atypical PKC-interacting protein p62 is an important mediator of RANK-activated osteoclastogenesis.** *Developm cell*. 2004;6:303-9.

115. Bitto A, Lerner CA, Nacarelli T, Crowe E, Torres C, Sell C. **p62/SQSTM1 at the interface of aging, autophagy, and disease**. *Age*. 2014;36:1123-37.

116. Kuusisto E, Salminen A, Alafuzoff I. **Ubiquitin-binding protein p62 is present in neuronal and glial inclusions in human tauopathies and synucleinopathies**. *Neuroreport*. 2001;12:2085-90.

117. Ramesh Babu J, Lamar Seibenhener M, Peng J, Strom A, Kemppainen R, Cox N, et al. **Genetic inactivation of p62 leads to accumulation of hyperphosphorylated tau and neurodegeneration**. *J Neurochem*. 2008;106:107-20.

118. Du Y, Wooten MC, Gearing M, Wooten MW. **Age-associated oxidative damage to the p62 promoter: implications for Alzheimer disease**. *Free Rad Biol and Med* 2009;46:492-501.

119. Lin MT, Beal MF. **Mitochondrial dysfunction and oxidative stress in neurodegenerative diseases**. *Nature*. 2006;443:787-95.

120. Johansen T, Lamark T. **Selective autophagy mediated by autophagic adapter proteins**. *Autophagy*. 2011;7:279-96.

121. Pankiv S, Clausen TH, Lamark T, Brech A, Bruun JA, Outzen H, et al. **p62/SQSTM1 binds directly to Atg8/LC3 to facilitate degradation of ubiquitinated protein aggregates by autophagy**. *J Biol Chem*. 2007;282:24131-45.

122. Matsumoto G, Wada K, Okuno M, Kurosawa M, Nukina N. **Serine 403 phosphorylation of p62/SQSTM1 regulates selective autophagic clearance of ubiquitinated proteins**. *Mol Cell*. 2011;44:279-89.

123. Kimura S, Noda T, Yoshimori T. **Dynein-dependent movement of autophagosomes mediates efficient encounters with lysosomes**. *Cell Struct Funct*. 2008;33:109-22.

124. Ravikumar B, Acevedo-Arozena A, Imarisio S, Berger Z, Vacher C, O'Kane CJ, et al. **Dynein mutations impair autophagic clearance of aggregate-prone proteins**. *Nat Genet*. 2005;37:771-6.

125. Tanaka Y, Guhde G, Suter A, Eskelinen E, Hartmann D, Lüllmann-Rauch R, et al. **Accumulation of autophagic vacuoles and cardiomyopathy in LAMP-2-deficient mice**. *Nature*. 2000;406:902-6.

126. Liang C, Lee J, Inn K, Gack MU, Li Q, Roberts EA, et al. **Beclin1-binding UVRAG targets the class C Vps complex to coordinate autophagosome maturation and endocytic trafficking**. *Nat Cell Biol*. 2008;10:776-87.

127. Kirisako T, Ichimura Y, Okada H, Kabeya Y, Mizushima N, Yoshimori T, et al. **The reversible modification regulates the membrane-binding state of Apg8/Aut7 essential for autophagy and the cytoplasm to vacuole targeting pathway**. *J Cell Biol*. 2000;151:263-76.

128. Yamamoto A, Tagawa Y, Yoshimori T, Moriyama Y, Masaki R, Tashiro Y. **Bafilomycin A1 prevents maturation of autophagic vacuoles by inhibiting fusion between autophagosomes and lysosomes in rat hepatoma cell line, H-4-II-E cells.** *Cell Struct Funct*. 1998;23:33-42.

129. Yang Q, Guan K. **Expanding mTOR signaling**. *Cell Res*. 2007;17:666-81.

130. Kim D, Sarbassov DD, Ali SM, King JE, Latek RR, Erdjument-Bromage H, et al. **mTOR interacts with raptor to form a nutrient-sensitive complex that signals to the cell growth machinery**. *Cell*. 2002;110:163-75.

131. Sarbassov dD, Ali SM, Sabatini DM. **Growing roles for the mTOR pathway**. *Curr Opin Cell Biol.* 2005;17:596-603.

132. Kim D, Sarbassov DD, Ali SM, King JE, Latek RR, Erdjument-Bromage H, et al. **mTOR interacts with raptor to form a nutrient-sensitive complex that signals to the cell growth machinery**. *Cell.* 2002;110:163-75.

133. Hosokawa N, Hara T, Kaizuka T, Kishi C, Takamura A, Miura Y, et al. **Nutrient-dependent mTORC1 association with the ULK1-Atg13-FIP200 complex required for autophagy**. *Mol Biol Cell*. 2009;20:1981-91.

134. Cantley LC. **The phosphoinositide 3-kinase pathway**. *Science*. 2002;296:1655-7.

136. Sarbassov DD, Ali SM, Sabatini DM. **Growing roles for the mTOR pathway**. *Curr Opin Cell Biol*. 2005;17:596-603.

137. Petiot A, Ogier-Denis E, Blommaart EF, Meijer AJ, Codogno P. **Distinct classes of phosphatidylinositol 3′-kinases are involved in signaling pathways that control macroautophagy in HT-29 cells.** *J Biol Chem*. 2000;275:992-8.

138. He C, Klionsky DJ. **Regulation mechanisms and signaling pathways of autophagy**. *Annu Rev Genet*. 2009;43:67-93.

139. Tracy K, Dibling BC, Spike BT, Knabb JR, Schumacker P, Macleod KF. **BNIP3 is an RB/E2F target gene required for hypoxia-induced autophagy**. *Mol Cell Biol.* 2007;27:6229-42.

140. Reiling JH, Hafen E. **The hypoxia-induced paralogs Scylla and Charybdis inhibit growth by down-regulating S6K activity upstream of TSC in Drosophila**. *Genes Dev*. 2004;18:2879-92.

141. Papandreou I, Lim A, Laderoute K, Denko N. **Hypoxia signals autophagy in tumor cells via AMPK activity, independent of HIF-1, BNIP3, and BNIP3L**. *Cell Death Differ*. 2008;15:1572-81.

142. Glunde K, Shah T, Winnard PT,Jr, Raman V, Takagi T, Vesuna F, et al. **Hypoxia regulates choline kinase expression through hypoxia-inducible factor-1 alpha signaling in a human prostate cancer model**. *Cancer Res*. 2008;68:172-80.

143. Bernales S, McDonald KL, Walter P. **Autophagy counterbalances endoplasmic reticulum expansion during the unfolded protein response**. *PLoS Biol*. 2006;4:e423.

144. Ma Y, Hendershot LM. **The unfolding tale of the unfolded protein response**. *Cell.* 2001;107:827-30.

145. Li J, Ni M, Lee B, Barron E, Hinton D, Lee A. **The unfolded protein response regulator GRP78/BiP is required for endoplasmic reticulum integrity and stress-induced autophagy in mammalian cells**. *Cell Death Differ.* 2008;15:1460-71.

146. Høyer-Hansen M, Bastholm L, Szyniarowski P, Campanella M, Szabadkai G, Farkas T, et al. **Control of macroautophagy by calcium, calmodulin-dependent kinase kinase-β, and Bcl-2**. *Mol Cell*. 2007;25:193-205.

147. Sakaki K, Wu J, Kaufman RJ. **Protein kinase Ctheta is required for autophagy in response to stress in the endoplasmic reticulum**. *J Biol Chem*. 2008;283:15370-80.

148. Marino G, Salvador-Montoliu N, Fueyo A, Knecht E, Mizushima N, Lopez-Otin C. **Tissue-specific autophagy alterations and increased tumorigenesis in mice deficient in Atg4C/autophagin-3**. *J Biol Chem*. 2007;282:18573-83.

149. Crighton D, Wilkinson S, O'Prey J, Syed N, Smith P, Harrison PR, et al. **DRAM, a p53-induced modulator of autophagy, is critical for apoptosis**. *Cell*. 2006;126:121-34.

150. Karantza-Wadsworth V, Patel S, Kravchuk O, Chen G, Mathew R, Jin S, et al. **Autophagy mitigates metabolic stress and genome damage in mammary tumorigenesis**. *Genes Dev*. 2007;21:1621-35.

151. Mathew R, Karp CM, Beaudoin B, Vuong N, Chen G, Chen H, et al. **Autophagy suppresses tumorigenesis through elimination of p62**. *Cell*. 2009;137:1062-75.

152. Sato K, Tsuchihara K, Fujii S, Sugiyama M, Goya T, Atomi Y, et al. **Autophagy is activated in colorectal cancer cells and contributes to the tolerance to nutrient deprivation**. *Cancer Res.* 2007;67:9677-84.

153. Tasdemir E, Maiuri MC, Galluzzi L, Vitale I, Djavaheri-Mergny M, D'Amelio M, et al. **Regulation of autophagy by cytoplasmic p53**. *Nat Cell Biol*. 2008;10:676-87.

154. Ito H, Daido S, Kanzawa T, Kondo S, Kondo Y. **Radiation-induced autophagy is associated with LC3 and its inhibition sensitizes malignant glioma cells**. *Int J Oncol.* 2005;26:1401-10.

155. Singh R, Kaushik S, Wang Y, Xiang Y, Novak I, Komatsu M, et al. **Autophagy regulates lipid metabolism**. *Nature*. 2009;458:1131-5.

156. Ding W, Li M, Chen X, Ni H, Lin C, Gao W, et al. **Autophagy reduces acute ethanol-induced hepatotoxicity and steatosis in mice**. *Gastroenterology*. 2010;139:1740-52.

157. Kihara A, Noda T, Ishihara N, Ohsumi Y. **Two distinct Vps34 phosphatidylinositol 3-kinase complexes function in autophagy and carboxypeptidase Y sorting in Saccharomyces cerevisiae**. *J Cell Biol*. 2001;152:519-30.

158. Feng Y, Yao Z, Klionsky DJ. **How to control self-digestion: transcriptional, post-transcriptional, and post-translational regulation of autophagy**. *Trends Cell Biol*. 2015;25:354-63.

159. Knævelsrud H, Simonsen A. **Lipids in autophagy: constituents, signaling molecules and cargo with relevance to disease**. *Biochimet Biophys Acta*. 2012;1821:1133-45.

160. Dooley HC, Razi M, Polson HE, Girardin SE, Wilson MI, Tooze SA. **WIPI2 links LC3 conjugation with PI3P, autophagosome formation, and pathogen clearance by recruiting Atg12–5-16L1**. *Mol Cell*. 2014;55:238-52.

161. Proikas-Cezanne T, Waddell S, Gaugel A, Frickey T, Lupas A, Nordheim A. **WIPI-1α (WIPI49), a member of the novel 7-bladed WIPI protein family, is aberrantly expressed in human cancer and is linked to starvation-induced autophagy**. *Oncogene*. 2004;23:9314-25.

162. Polson HE, de Lartigue J, Rigden DJ, Reedijk M, Urbé S, Clague MJ, et al. **Mammalian Atg18 (WIPI2) localizes to omegasome-anchored phagophores and positively regulates LC3 lipidation**. *Autophagy*. 2010;6:506-22.

163. Simonsen A, Birkeland HC, Gillooly DJ, Mizushima N, Kuma A, Yoshimori T, et al. **Alfy, a novel FYVE-domain-containing protein associated with protein granules and autophagic membranes**. *J Cell Sci.* 2004;117:4239-51.

164. Clausen TH, Lamark T, Isakson P, Finley KD, Larsen KB, Brech A, et al. **p62/SQSTM1 and ALFY interact to facilitate the formation of p62 bodies/ALIS and their degradation by autophagy**. *Autophagy*. 2010;6:330-44.

165. Schink KO, Raiborg C, Stenmark H. **Phosphatidylinositol 3-phosphate, a lipid that regulates membrane dynamics, protein sorting and cell signalling**. *Bioessays*. 2013;35:900-12.

166. Vergne I, Roberts E, Elmaoued RA, Tosch V, Delgado MA, Proikas-Cezanne T, et al. **Control of autophagy initiation by phosphoinositide 3-phosphatase Jumpy**. *EMBO J.* 2009;28:2244-58.

167. Papp D, Kovács T, Billes V, Varga M, Tarnóci A, Hackler Jr L, et al. **AUTEN-67, an autophagy-enhancing drug candidate with potent antiaging and neuroprotective effects**. *Autophagy*. 2016;12:273-86.

168. Chen D, Fan W, Lu Y, Ding X, Chen S, Zhong Q. **A mammalian autophagosome maturation mechanism mediated by TECPR1 and the Atg12-Atg5 conjugate**. *Mol Cell.* 2012;45:629-41.

169. Voelker DR. **Organelle biogenesis and intracellular lipid transport in eukaryotes.** *Microbiol Rev*. 1999;55:543-60.

170. Fang Y, Vilella-Bach M, Bachmann R, Flanigan A, Chen J. **Phosphatidic acid-mediated mitogenic activation of mTOR signaling**. *Science*. 2001;294:1942-5.

171. Jang Y, Choi K, Min D. **Phospholipase D-mediated autophagic regulation is a potential target for cancer therapy**. *Cell Death & Differ*. 2014;21:533-46.

172. Dall'Armi C, Hurtado-Lorenzo A, Tian H, Morel E, Nezu A, Chan RB, et al. **The phospholipase D1 pathway modulates macroautophagy**. *Nature Commu* 2010;1:142.

173. Rashid A, Pizer ES, Moga M, Milgraum LZ, Zahurak M, Pasternack GR, et al. **Elevated expression of fatty acid synthase and fatty acid synthetic activity in colorectal neoplasia**. *Am J Pathol*. 1997;150:201-8.

174. Glunde K, Bhujwalla ZM, Ronen SM. **Choline metabolism in malignant transformation.** *Nat Rev Cancer*. 2011;11:835-48.

175. Geng Y, Kohli L, Klocke BJ, Roth KA. **Chloroquine-induced autophagic vacuole accumulation and cell death in glioma cells is p53 independent**. *Neuro Oncol.* 2010;12:473-81.

176. Lock R, Roy S, Kenific CM, Su JS, Salas E, Ronen SM, et al. **Autophagy facilitates glycolysis during Ras-mediated oncogenic transformation.** *Mol Biol Cell*. 2011;22:165-78.

177. Buick RN, Filmus J, Quaroni A. **Activated H-ras transforms rat intestinal epithelial cells with expression of α-TGF.** *Exp Cell Res*. 1987;170:300-9.

178. Rak J, Mitsuhashi Y, Erdos V, Huang SN, Filmus J, Kerbel RS. **Massive programmed cell death in intestinal epithelial cells induced by three-dimensional growth conditions: suppression by mutant c-H-ras oncogene expression**. *J Cell Biol*. 1995;131:1587-98.

179. Fung C, Lock R, Gao S, Salas E, Debnath J. **Induction of autophagy during extracellular matrix detachment promotes cell survival**. *Mol Biol Cell.* 2008;19:797-806.

180. Frisch SM, Francis H. **Disruption of epithelial cell-matrix interactions induces apoptosis**. *J Cell Biol*. 1994;124:619-26.

181. Yoo BH, Wu X, Li Y, Haniff M, Sasazuki T, Shirasawa S, et al. **Oncogenic ras-induced down-regulation of autophagy mediator Beclin-1 is required for malignant transformation of intestinal epithelial cells**. *J Biol Chem*. 2010;285:5438-49.

182. Boya P, Gonzalez-Polo RA, Casares N, Perfettini JL, Dessen P, Larochette N, et al. **Inhibition of macroautophagy triggers apoptosis.** *Mol Cell Biol.* 2005;25:1025-40.

183. Chaitanya GV, Alexander JS, Babu PP. **PARP-1 cleavage fragments: signatures of cell-death proteases in neurodegeneration**. *Cell Commun and Sign*. 2010;8:1.

184. Morita Y, Sakaguchi T, Ikegami K, Goto-Inoue N, Hayasaka T, Hang VT, et al. **Lysophosphatidylcholine acyltransferase 1 altered phospholipid composition and regulated hepatoma progression**. *J Hepatol*. 2013;59:292-9.

185. Zhou X, Lawrence TJ, He Z, Pound CR, Mao J, Bigler SA. **The expression level of lysophosphatidylcholine acyltransferase 1 (LPCAT1) correlates to the progression of prostate cancer**. *Exp Mol Pathol*. 2012;92:105-10.

186. Guo JY, Chen HY, Mathew R, Fan J, Strohecker AM, Karsli-Uzunbas G, et al. **Activated Ras requires autophagy to maintain oxidative metabolism and tumorigenesis**. *Genes Dev*. 2011;25:460-70.

187. Wirawan E, Walle LV, Kersse K, Cornelis S, Claerhout S, Vanoverberghe I, et al. **Caspase-mediated cleavage of Beclin-1 inactivates Beclin-1-induced autophagy and enhances apoptosis by promoting the release of proapoptotic factors from mitochondria**. *Cell Death Dis*. 2010;1:e18.

188. Li H, Wang P, Yu J, Zhang L. **Cleaving Beclin 1 to suppress autophagy in chemotherapy-induced apoptosis**. *Autophagy.* 2011;7:1239-1241.

189. Zeisel, S. H. **Metabolic crosstalk between choline/1-carbon metabolism and energy homeostasis**. *Clin. Chem.Lab. Med*. 2013;*51*:467-475.